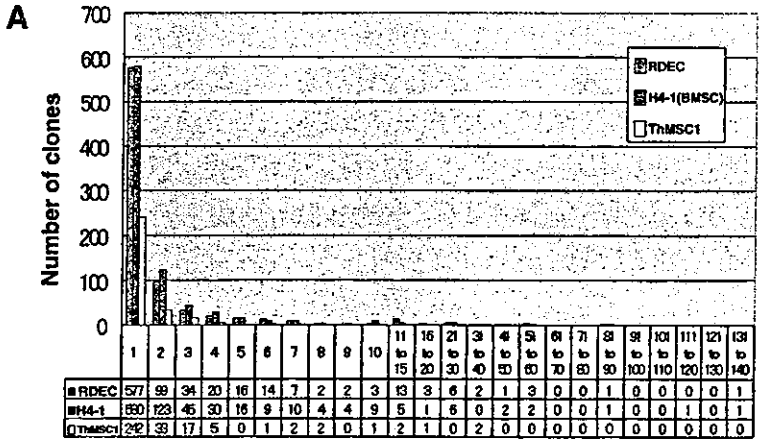

	1	2	3	4	5	6	7	8	9	10	11 to 15	16 to 20	21 to 30	31 to 40	41 to 50	51 to 60	61 to 70	71 to 80	81 to 90	91 to 100	101 to 110	111 to 120	121 to 130	131 to 140
RDEC	577	99	34	20	16	14	7	2	2	3	13	3	6	2	1	3	0	0	1	0	0	0	0	1
H4-1	660	123	45	30	16	9	10	4	4	9	5	1	6	0	2	2	0	0	1	0	0	1	0	1
ThMSC1	242	33	17	5	0	1	2	2	0	1	2	1	0	2	0	0	0	0	0	0	0	0	0	0

B

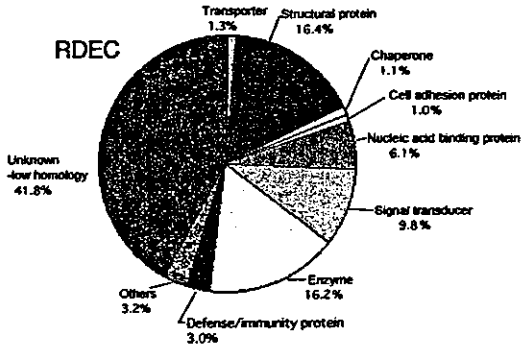

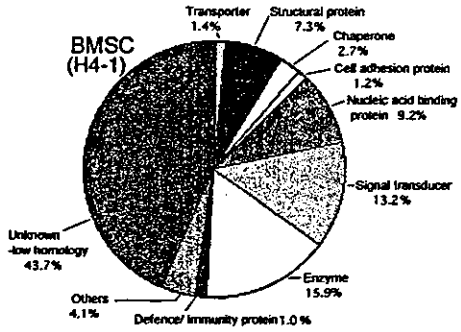

category of molecular function	RDEC	BMSC	ThMSC1
transporter	1.3%	1.4%	2.1%
structural protein	16.4%	7.3%	7.5%
chaperone	1.1%	2.7%	2.5%
cell adhesion protein	1.0%	1.2%	1.0%
nucleic acid binding protein	6.1%	9.3%	8.6%
signal transducer	9.8%	13.2%	13.9%
enzyme	16.2%	15.9%	15.4%
apoptosis	0.1%	0.3%	0.2%
defense/immunity protein	3.0%	1.0%	1.0%
others	3.2%	4.1%	3.4%
unknown low homology	41.8%	43.7%	44.4%

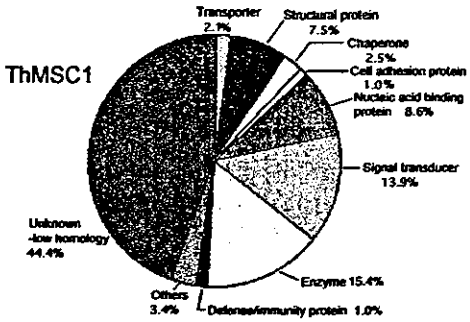

C

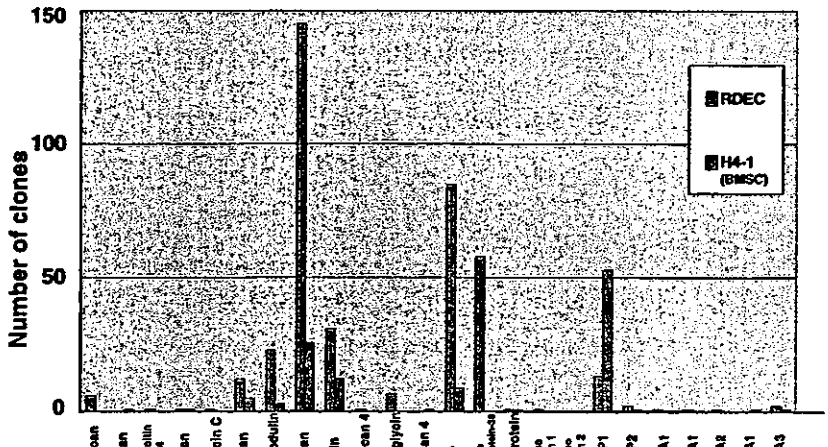

	Aggrecan	Versican	Chondrolin sulfate 4	Tesitcan	Tenascin C	Lumican	Fibromodulin	Biglycan	Decorin	Syndecan 4	Osteoglycin	Glypican 4	COMP	Cartilage glycoprotein	Link protein	Thrombospondin 1	Thrombospondin 2	EFEMP1	EFEMP2	Col 1 A1	Col 3 A1	Col 6 A2	Col 6 A1	Col 6 A3	Total
RDEC	6	0	1	1	1	12	23	145	38	1	7	0	85	58	1	1	0	13	2	1	1	1	0	2	393
H4-1	0	1	0	1	0	5	3	33	12	0	0	1	9	0	1	0	0	53	1	0	0	0	1	1	115

Table 4
The 15 most highly expressed genes in the cDNA library for RDEC, H4-1 (BMSC), and ThMSC1 cells[a]

Ranking	Gene title	Gene symbol	Gene ID	Identity	Clones	Expression level
RDEC						
1	Biglycan	BGN	NM_001711.1	100%	145	5.50%
2	Transforming growth factor, beta-induced	TGFBI	NM_000358.1	100%	133	5.06%
3	Cartilage oligomeric matrix protein	COMP	NM_000095.1	98%	85	3.24%
4	Chitinase 3-like 1	CHI3L1	NM_001276.1	99%	58	2.21%
5	Complement component 1, r subcomponent	C1R	NM_001733.1	99%	51	1.94%
6	Decidual protein induced by progesterone	DEPP	NM_007021.1	100%	41	1.56%
7	Procollagen-proline, 2-oxoglutarate 4-dioxygenase	P4HB	NM_000918.1	97%	32	1.22%
8	Decorin	DCN	NM_001920.1	99%	31	1.18%
9	Insulin-like growth factor binding protein 3	IGFBP3	NM_000598.1	97%	30	1.14%
10	Vimentin	VIM	NM_003380.1	100%	28	1.07%
11	Heat shock 70-kDa protein 8	HSPA8	NM_006597.1	99%	27	1.03%
12	Lamin A/C	LMNA	NM_005572.1	99%	23	0.88%
12	Fibromodulin	FMOD	NM_002023.2	98%	23	0.88%
14	Pyruvate kinase, muscle	PKM2	NM_002654.1	99%	21	0.80%
15	Granulin	GRN	NM_002087.1	100%	20	0.76%
H4-1 (BMSC)						
1	Insulin-like growth factor binding protein-3	IGFBP3	NM_000598.1	97%	131	4.88%
2	Transforming growth factor, beta-induced	TGFBI	NM_000358.1	100%	119	4.43%
3	Eukaryotic translation elongation factor-1 alpha 1	EEF1A1	NM_001402.1	99%	88	3.28%
4	Proteinase inhibitor, clade H (heat shock protein 47)	SERPINH2	NM_001235.1	99%	56	2.08%
5	EGF-containing fibulin-like extracellular matrix protein 1	EFEMP1	NM_004105.2	99%	53	1.97%
6	Vimentin	VIM	NM_003380.1	100%	43	1.60%
7	Heat shock 70-kDa protein 8	HSPA8	NM_006597.1	99%	42	1.56%
8	Actin, beta	ACTB	NM_001101.2	99%	27	1.00%
9	Biglycan	BGN	NM_001711.1	100%	26	0.97%
9	Procollagen-proline, 2-oxoglutarate 4-dioxygenase	P4HB	NM_000918.1	97%	26	0.97%
11	Connective tissue growth factor	CTGF	NM_001901.1	98%	24	0.89%
12	Amyloid beta (A4) precursor-like protein 2	APLP2	NM_001642.1	99%	21	0.78%
13	Lamin A/C	LMNA	NM_005572.1	99%	20	0.74%
14	Pyruvate kinase, muscle	PKM2	NM_002654.1	99%	15	0.56%
14	Complement component 1, r subcomponent	C1R	NM_001733.1	99%	12	0.45%
15	Decorin	DCN	NM_001920.1	99%	12	0.45%
ThMSC1						
1	Insulin-like growth factor binding protein 3	IGFBP3	NM_000598.1	97%	37	5.51%
2	Transforming growth factor, beta-induced	IGFBI	NM_000358.1	100%	36	5.37%
3	Vimentin	VIM	NM_003380.1	100%	19	2.83%
4	Eukaryotic translation elongation factor-1 alpha 1	EEF1A1	NM_001402.1	99%	12	1.79%
4	Heat shock 70-kDa protein 8	HSPA8	NM_006597.1	99%	12	1.79%
6	EGF-containing fibulin-like extracellular matrix protein 1	EFEMP1	NM_004105.2	99%	10	1.49%
7	Lactate dehydrogenase A	LDHA	NM_005566.1	99%	8	1.19%
7	Lamin A/C	LMNA	NM_005572.1	99%	8	1.19%
9	Biglycan	BGN	NM_001711.1	100%	7	1.04%
10	Pyruvate kinase, muscle	PKM2	NM_002654.1	99%	6	1.04%
11	Upregulated by 1.25-dihydroxyvitamin D-3	VDUP1	NM_006472.1	99%	4	0.60%
11	Immunoglobulin superfamily containing leucine-rich repeat	ISLR	NM_005545.1	100%	4	0.60%
11	P311 protein	P311	NM_004772.1	99%	4	0.60%
11	RAP1B, member of RAS oncogene family	RAP1B	NM_015646.1	98%	4	0.60%
11	Karyopherin alpha 2	KPNA2	NM_002266.1	99%	4	0.60%

[a] RDEC, redifferentiation of dedifferentiated chondrocytes; BMSC, bone marrow stromal cells; EGF, epidermal growth factor.

Fig. 5. General analysis of cDNA library from redifferentiated dedifferentiated chondrocytes (DEC), bone marrow stromal cells H-1 (BMSC), and ThMSC1. (A) The number of clones per unigene cluster that belongs to high similarity (identity over 96%). Approximately 70% of redifferentiated DEC (RDEC) and H4-1 clones (BMSC) was a single clone. For ThMSC1, 242 clones (78%) were nonrepetitive clones. (B) Distribution of the molecular functions of clones for redifferentiated DEC (RDEC), H4-1 (BMSC), and ThMSC1. Each slice lists the numbers and percentages of human gene functions assigned to a given category of molecular function according to the Gene Ontology (GO). (C) The number of clones on extracellular matrix genes for redifferentiated DEC (RDEC) and H4-1 (BMSC).

Table 5
The genes (identity over 96% of similarity) with the classification of molecular function[a]

Classification	Subclassification	Gene title	Gene symbol	Gene ID	Identity	RDEC	H4-1	ThMSC1
Extracellular matrix	Proteoglycan	Aggrecan	PG1	NM_001135.1	99%	6	0	0
		Versican	PG2	NM_004385.1	99%	0	1	0
		Chondroitin sulfate 4	CSPG4	NM_001897.1	100%	1	0	0
		Testican	SPOCK	NM_004598.2	99%	1	1	0
		Tenascin C	HXB	NM_002160.1	99%	1	0	0
		Lumican	LUM	NM_002345.1	99%	12	5	1
		Fibromudulin	FMOD	NM_002023.2	98%	23	3	0
		Biglycan	BGN	NM_001711.1	100%	145	26	7
		Decorin	DCN	NM_001920.1	99%	31	12	3
		Syndecan4	SDC4	NM_002999.1	100%	1	0	0
		Osteoglycin	OGN	NM_033014.1	99%	7	0	0
		Glypican 4	GPN4	NM_001448.1	99%	0	1	0
	Matrix protein	Cartilage oligomeric matrix protein	COMP	NM_000095.1	98%	85	9	1
		Cartilage glycoprotein-39	CHI3L1	NM_001276.1	99%	58	0	0
		Cartilage linking protein 1	CRTL1	NM_001884.1	99%	1	1	1
		Thrombospondin 1	THBS1	NM_006988.2	100%	1	0	0
		Thrombospondin 2	THBS2	NM_003247.1	100%	0	0	0
		EGF-containing fibulin-like Extracellular matrix protein 1	EFEMP1	NM_004105.2	99%	13	53	0
		EGF-containing fibulin-like Extracellular matrix protein 2	EFEMP2	NM_016938.1	99%	2	1	0
	Collagen	Collagen, type I, α1	COL1A1	NM_000088.2	99%	1	0	0
		Collagen, type III, α1	COL3A1	NM_000090.2	100%	1	0	0
		Collagen, type V, α2	COL5A2	NM_000393.1	99%	1	0	0
		Collagen, type VI, α1	COL6A1	NM_001848.1	99%	0	1	0
		Collagen, type VI, α3	COL6A3	NM_004369.1	99%	2	1	0
Growth factor	Growth factor	Transforming growth factor, β1	TGFb1	NM_000660.1	99%	1	0	0
		Fibroblast growth factor 7	FGF7	NM_002009.2	100%	1	7	1
		Vascular endothelial growth factor	VEGF	NM_003376.1	100%	1	0	0
		Vascular endothelial growth factor C	VEGFC	NM_005429.1	100%	1	0	0
		Growth differentiation factor 10	GDF10	NM_004962.2	99%	1	0	0
		Connective tissue growth factor	CTGF	NM_001901.1	98%	0	24	3
		Platelet-derived growth factor C	PDGFC	NM_016205.1	100%	1	1	0
		Heparin-binding epidermal growth factor-like growth factor	DTR	NM_001945.1	99%	0	0	1
		Granulin	GRN	NM_002087.1	100%	20	7	1
Growth factor-related protein		Transforming growth factor, β-induced	TGFB11	NM_000358.1	100%	133	119	36
		Insulin-like growth factor binding protein 3	IGFBP3	NM_000598.1	97%	30	131	37
		Gremlin	CKTSF1B1	NM_013372.1	99%	0	5	0
CCN family		WNT1 inducible signaling pathway protein 1	WISP1	NM_003882.1	99%	0	1	0
		WNT1 inducible signaling pathway protein 2	WISP2	NM_003881.1	99%	0	1	0
Wnt	Wnt family	Wingless-type MMTV integration site family, member 5A	WNT5A	NM_003392.1	98%	1	0	0
	Wnt signal pathway	Frizzled-related protein	FRZB	NM_001463.1	98%	5	0	0
		Dickkopf homolog 3	DKK3	NM_013253.1	100%	2	0	0
Cell surface markers		10	CALLA	NM_007288.1	99%	0	1	0
		24		NM_013230.1	99%	0	1	0
		29		NM_002211.1	100%	2	3	0
		44	H-CAM, Pgp-1	NM_000610.1	99%	11	7	2
		46	MCP	NM_002389.1	99%	1	0	0
		54	ICAM11	NM_000201.1	100%	1	0	0
		55	DAF	NM_000574.1	100%	1	1	1
		59		NM_000611.1	99%	1	5	2
		68		NM_001251.1	100%	1	0	0
		73		NM_002526.1	99%	0	1	0
		90	Thy-1	NM_002526.1	99%	4	2	1
		97	GR1	NM_001784.1	100%	0	1	01
		105	ENG	NM_000118.1	100%	4	5	1
		164	MGC-24	NM_006016.1	100%	0	2	

Table 5 (*continued*)

Classification	Subclassification	Gene title	Gene symbol	Gene ID	Identity	RDEC	H4-1	ThMSC1
Cell adhesions	Integrin	Integrin, α5	ITGA5	NM_002205.1	100%	0	3	0
		Integrin, α11	ITGa11	NM_012211.1	100%	1	0	0
		Integrin, β1	ITGB1	NM_002211.1	98%	2	3	0
		Integrin, β-like 1	ITGBL1	NM_004791.1	99%	0	0	0
		Integrin, β2	ITGB2	NM_000211.1	99%	0	0	1
		Integrin, β5	ITGB5	NM_002213.1	100%	1	0	0
	Cadherin	Cadherin 11	CDH11	NM_001797.1	100%	1	1	0
		Cadherin 13	CDH13	NM_001257.1	98%	0	2	1
	Cell adhesion molecules	Cerebral cell adhesion molecule	C-CAM	NM_016174.1	99%	1	0	0
		Vascular cell adhesion molecule 1	VCAM1	NM_001078.1	99%	0	1	2
		Junctional adhesion molecule 3	JAM3	NM_031470.1	100%	1	0	0
		Melanoma adhesion molecule	MCAM	NM_006500.1	99%	0	1	0
		Intercellular adhesion molecule 1	ICAM1	NM_000201.1	100%	1	0	0
		Intercellular adhesion molecule 3	ICAM3	NM_002162.2	98%	0	0	0
MMP	MMP	Matrix metalloproteinase 1	MMP1	NM_002421.2	99%	4	0	0
		Matrix metalloproteinase 2	MMP2	NM_004530.1	99%	7	2	0
		Matrix metalloproteinase 3	MMP3	NM_002422.2	100%	3	0	0
		Matrix metalloproteinase 14	MMP14	NM_004995.2	99%	0	0	0
TIMP	TIMP	Tissue inhibitor of metalloproteinase 1	TIMP1	NM_003254.1	99%	2	0	0
		Tissue inhibitor of metalloproteinase 3	TIMP3	NM_000362.2	98%	2	2	0
ADAM	ADAM	A disintegrin-like and metalloprotease with thrombospondin type 1 motif, 1	ADAMTS1	NM_006988.2	99%	0	0	0
		A disintegrin and metalloproteinase domain 9	ADAM9	NM_003816.1	99%	0	1	0
		A disintegrin and metalloproteinase domain 10	ADAM10	NM_001110.1	99%	0	0	0
		A disintegrin and metalloproteinase domain 15	ADAM15	NM_003815.2	99%	2	0	0
Receptor	Type I	Interleukin 6 signal transducer	IL6ST	NM_002184.1	99%	1	0	0
		Oncostatin M receptor	OSM	NM_003999.1	99%	3	0	0
		Interleukin 13 receptor, α1	IL13RA1	NM_001560.1	100%	1	0	0
	Type II	Interferon-γ receptor 1	IFNrR1	NM_000416.1	100%	0	2	0
	Type III	Tumor necrosis factor receptor superfamily, member 1A	TNFRSF1A	NM_001065.1	99%	4	5	2
		Tumor necrosis factor receptor superfamily, member 10d	TNFRSF10D	NM_003840.1	100%	1	0	0
		Tumor necrosis factor receptor superfamily, member 10b	TNFRSF10B	NM_003842.1	100%	1	1	0
		Lymphotoxin β receptor (TNFR superfamily, member 3)	LTBR	NM_002342.1	100%	0	0	0
	Other (inner cellular)	Retinoic acid receptor, γ	RARG	NM_000966.1	100%	2	0	0
Transcription	ETS	V-ets avian erythroblastosis virus E26 oncogene homolog 2	ETS2	NM_005239.1	100%	2	0	0
		Ets variant gene 5	ETV5	NM_004454.1	98%	0	0	0
		V-ets avian erythroblastosis virus E26 oncogene related	ERG	NM_004449.2	100%	1	0	0
SOX	SOX	SRY (sex determining region)-box 9	SOX9	NM_000346.1	99%	1	0	0

[a] EGF, epidermal growth factor.

Expression of cartilage-related genes in DECs and BMSCs

The results of RT-PCR assays of parallel samples were consistent with the cDNA profiling data (Fig. 6). The expression of the COMP genes was detected at a higher level in the redifferentiated DECs than in H4-1 cells (Fig. 6A), and expression of cartilage glycoprotein-39 was found in both DECs and redifferentiated DECs (Fig. 6B). Expression of WISP1 was observed in H4-1 cells but not in DECs or redifferentiated DECs (Fig. 6C).

Discussion

BMSCs were successfully cultured for more than 25 passages. H4-1 cells proliferated and retained differentiation capability even after 48 population doublings

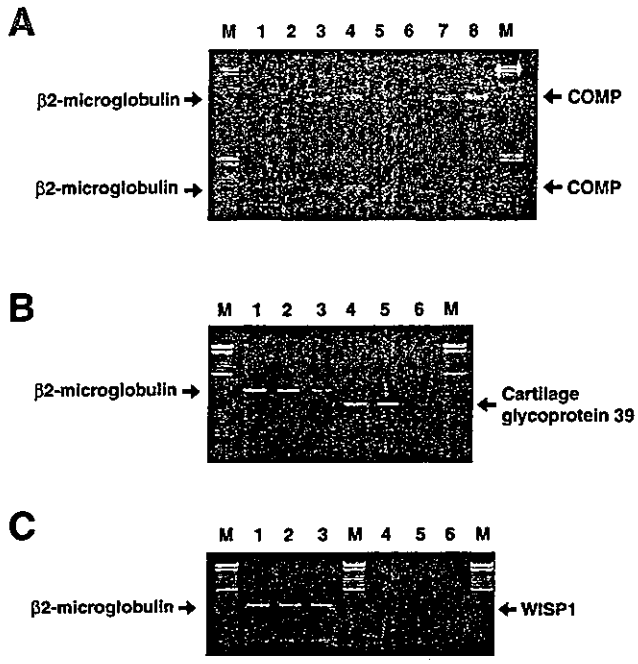

Fig. 6. The expression pattern of cartilage-related gene was consistent with the results of random sequencing analysis. (A) Reverse transcription-polymerase chain reaction (RT-PCR) analysis of cartilage oligomeric matrix protein (COMP) expression (lanes 5–8) in redifferentiation of dedifferentiated chondrocytes (DEC) at 1 week (upper column) and in the monolayer culture of H4-1 (lower column). Expression of β2-microglobulin is used for an internal control of each RNA (lanes 1–4). Lanes 1 and 5, 20 cycles of PCR; lanes 2 and 6, 25 cycles; lanes 3 and 7, 30 cycles; lanes 4 and 8, 35 cycles. (B and C) RT-PCR analysis of cartilage glycoprotein-39 (B) and WISP 1 (C). M, molecular markers; lanes 1 and 4, monolayer culture of DEC; lanes 2 and 5, redifferentiation of DEC at 1 week, lanes 3 and 6, monolayer culture of H4-1.

(PDs), while most marrow-derived mesenchymal cells reached senescence before 30 PDs. Human marrow progenitor cells have been successfully cultured for more than 60 cell doublings with multipotency under specific culture conditions [31]. H4-1 cells had a surface marker pattern similar to that of mesodermal progenitor cells, and thus it is of interest to investigate whether it undergoes not only chondrogenic differentiation but differentiation into other mesenchymal phenotypes under specific inducing conditions.

The method of chondrosphere formation, which has been modified in this study, promoted redifferentiation of dedifferentiated chondrocytes. Pellet culture is the method most commonly used for chondrogenesis of marrow mesenchymal stem cells [15], and comparison of the chondrosphere culture method and pellet method revealed that they have similar effects in inducting chondrogenesis in vitro in terms of increasing cell density to a high level. Based on the evidence that chondrocytes markers such as aggrecan and type II collagen were rapidly induced, 2-h cell aggregation by the chondrosphere method sufficiently promoted differentiation. Furthermore, since extremely abundant ECM was produced by the cultured cells, the chondrosphere culture did not require a scaffold for chondrogenesis. We conclude that chondrosphere formation is sufficient for chondrogenesis of dedifferentiated chondrocytes and H4-1 cells.

Human mesenchymal stem cells have been successfully isolated and can differentiate into osteocytes, chondrocytes, and adipocytes [15]. The surface antigen phenotype of H4-1 cells, c-kit negative and CD140α low or negative cells, showed differences from the surface antigens of human mesenchymal stem cells [15,31]. When FACS sorting is set for this population, $CD34^-$, $c\text{-}kit^-$, and $CD140\alpha^{-\text{ or low}}$, the fraction of human bone marrow cells will be highly enriched in chondrogenic progenitor cells. CD29, CD44, CD90, CD105, CD106, and CD166 were detected in both H4-1 cells and DECs in this study.

The consistency between the result of flow cytometric analysis and the frequency of the clusters (Table 6) indicates that the expression profiling by large-scale sequence analysis of the cDNA libraries obtained by oligocapping method [32] is valid, the same as previously reported large-scale sequencing analyses [33,34] and expression tag analyses [35]. Expression of "structural protein" on Gene Ontology, including the ECM, was much higher by redifferentiated DECs than by H4-1 and ThMSC1 cells, implying that the cells are mainly engaged in synthesizing ECM. Leucine-rich small proteoglycans having a molecular weight of 30 to 50 kDa include decorin, biglycan, fibromodulin, and lumican. Redifferentiated chondrocytes rapidly produced these small proteoglycans to embed themselves in the ECM, and

Table 6
Consistency between frequency of the clones and flow cytometric analysis[a]

Surface marker	H4-1 (BMSC)		Dedifferentiated chondrocytes	
	Flow cytometric analysis (folds)	cDNA analysis (clones)	Flow cytometric analysis (folds)	cDNA analysis (clones)
CD14	1	0	3	0
CD29	10	5	90	2
CD34	1	0	1	0
CD44	33	7	300	12
CD45	1	0	1	0
CD105	3	5	7	4
CD144	1	0	1	0
CD31	1	0	1	0
CD50	1	0	1	0
CD117	1	0	1	0
CD140a	1	1	2	1
CD90	5	2	43	4
CD106	5	1	6	0

[a] H4-1 (flow cytometric analysis), H4-1 (cDNA analysis), and dedifferentiated chondrocytes (flow cytometric analysis) were in the monolayer culture. Dedifferentiated chondrocytes (cDNA analysis) were in the condition of chondrosphere culture. BMSC, bone marrow stromal cells.

produced larger molecular weight proteoglycans, such as aggrecan at a later stage of differentiation. This pattern of expression for proteoglycans in redifferentiated DECs resembles the higher expression of biglycan, decorin, and fibromodulin by human mesenchymal stem cells by the pellet culture protocol [25].

Elongation factor 1 α1 (EF-1 α) is one of the highly expressed genes among "nucleic acid binding proteins" (88 clones in H4-1 cells and 15 clones in redifferentiated DECs). The marked difference between these H4-1 cells and DECs may be attributable to a stage of cellular aging, since the level of EF-1 α expression during aging, e.g., an irreversible decrease in EF-1 α, is found in aged mesenchymal cells [36,37]. Among growth factors, genes of the CCN family, including CTGF, WISP1 (CCN4), and WISP2 (CCN5), were highly detected in H4-1. WISP1 and WISP2 are expressed at high levels in fibroblasts, and overexpressed in colon tumors [38]. The proteins they encode bind to decorin and biglycan, and may prevent the inhibitory activity of decorin and biglycan. The next most highly expressed genes of growth factors in H4-1 cells were FGF7/keratinocyte growth factor. This growth factor has a mitogen potentiality for epithelial cells, but for neither fibroblasts nor endothelial cells [39]. One of the growth factor-related genes is gremlin, whose protein acts as an antagonist of BMP signaling by preventing BMPs from interacting with their receptors [40,41]. Gremlin was highly detected during the growth phase of H4-1 cells, and this protein may inhibit differentiation of these cells through BMP inhibition at this stage.

The expression pattern of chondrocyte-specific genes in dedifferentiated chondrocytes is different from that of ATDC5 cells, which are a mouse embryonal carcinoma-derived chondrogenic cell line. ATDC5 cells exhibit a multistep differentiation process encompassing the stages from chondrogenesis to enchondral ossification [42]. Early-phase differentiation is characterized by expression of type II collagen, followed by induction of the aggrecan gene [42]. Late-stage differentiation is characterized by the start of expression of short-chain collagen type X genes. By contrast, marrow-derived mesenchymal stem cells express the aggrecan genes at an early stage and then type II collagen during chondrogenic differentiation [15]. The time course of ECM expression in redifferentiated DECs in this study resembles that of mesenchymal stem cells during chondrogenic differentiation rather than that of differentiating embryonal cell carcinoma cells.

These established human mesenchymal cells with expression profiling provide a powerful model for a study of chondrogenic differentiation and our further understanding of cartilage regeneration using redifferentiated DECs and BMSCs. BMSCs with a chondrogenic potential and dedifferentiated chondrocytes are useful candidate cell sources for transplantation in osteoarthritis and rheumatoid arthritis.

Acknowledgments

We express our sincere thanks to K. Sakurada and Y. Yamada (Kyowa Hakko Kogyo Co., Ltd.) for their support throughout the work, to A. Wakamatsu for construction of the cDNA libraries and sequencing analysis, to S. Ishii, J. Yamamoto, K. Saito, and Y. Kawai for sequencing analysis, and to T. Inomata, Y. Setoyama, and N. Onoda for providing expert technical assistance. The study was supported in part by Health and Labour Sciences Research Grants, Translational Research from Ministry of Health Labour and Welfare, and a special grant for Advanced Research on Cancer from the Ministry of Education, Culture, Sports, Science, and Technology of Japan to T.K. and A.U.

References

[1] M. Solursh, Differentiation of cartilage and bone, Curr. Opin. Cell Biol. 1 (1989) 989–994.
[2] H.J. Hauselmann, R.J. Fernandes, S.S. Mok, T.M. Schmid, J.A. Block, M.B. Aydelotte, K.E. Kuettner, E.J. Thonar, Phenotypic stability of bovine articular chondrocytes after long-term culture in alginate beads, J. Cell Sci. 107 (1994) 17–27.
[3] A.M. Reginato, R.V. Iozzo, S.A. Jimenez, Formation of nodular structures resembling mature articular cartilage in long-term primary cultures of human fetal epiphyseal chondrocytes on a hydrogel substrate, Arthritis Rheum. 37 (1994) 1338–1349.
[4] C.W. Archer, J. McDowell, M.T. Bayliss, M.D. Stephens, G. Bentley, Phenotypic modulation in sub-populations of human articular chondrocytes in vitro, J. Cell Sci. 97 (Pt 2) (1990) 361–371.
[5] P.D. Benya, S.R. Padilla, M.E. Nimni, Independent regulation of collagen types by chondrocytes during the loss of differentiated function in culture, Cell 15 (1978) 1313–1321.
[6] P.D. Benya, J.D. Shaffer, Dedifferentiated chondrocytes reexpress the differentiated collagen phenotype when cultured in agarose gels, Cell 30 (1982) 215–224.
[7] V. Lefebvre, C. Peeters-Joris, G. Vaes, Production of collagens, collagenase and collagenase inhibitor during the dedifferentiation of articular chondrocytes by serial subcultures, Biochim. Biophys. Acta 1051 (1990) 266–275.
[8] J. Bonaventure, N. Kadhom, L. Cohen-Solal, K.H. Ng, J. Bourguignon, C. Lasselin, P. Freisinger, Reexpression of cartilage-specific genes by dedifferentiated human articular chondrocytes cultured in alginate beads, Exp. Cell Res. 212 (1994) 97–104.
[9] Y.M. Yoon, S.J. Kim, C.D. Oh, J.W. Ju, W.K. Song, Y.J. Yoo, T.L. Huh, J.S. Chun, Maintenance of differentiated phenotype of articular chondrocytes by protein kinase C and extracellular signal-regulated protein kinase, J. Biol. Chem. 277 (2002) 8412–8420.
[10] S.E. Haynesworth, M.A. Baber, A.I. Caplan, Cell surface antigens on human marrow-derived mesenchymal cells are detected by monoclonal antibodies, Bone 13 (1992) 69–80.
[11] N. Jaiswal, S.E. Haynesworth, A.I. Caplan, S.P. Bruder, Osteogenic differentiation of purified, culture-expanded human mesenchymal stem cells in vitro, J. Cell. Biochem. 64 (1997) 295–312.
[12] B. Johnstone, T.M. Hering, A.I. Caplan, V.M. Goldberg, J.U. Yoo, In vitro chondrogenesis of bone marrow-derived mesenchymal progenitor cells, Exp. Cell Res. 238 (1998) 265–272.
[13] A.M. Mackay, S.C. Beck, J.M. Murphy, F.P. Barry, C.O. Chichester, M.F. Pittenger, Chondrogenic differentiation of cultured human mesenchymal stem cells from marrow, Tissue Eng. 4 (1998) 415–428.
[14] J.E. Dennis, S.E. Haynesworth, R.G. Young, A.I. Caplan, Osteogenesis in marrow-derived mesenchymal cell porous ceramic composites transplanted subcutaneously: effect of fibronectin and laminin on cell

retention and rate of osteogenic expression, Cell Transplant. 1 (1992) 23–32.
[15] M.F. Pittenger, A.M. Mackay, S.C. Beck, R.K. Jaiswal, R. Douglas, J.D. Mosca, M.A. Moorman, D.W. Simonetti, S. Craig, D.R. Marshak, Multilineage potential of adult human mesenchymal stem cells, Science 284 (1999) 143–147.
[16] S. Wakitani, T. Goto, S.J. Pineda, R.G. Young, J.M. Mansour, A.I. Caplan, V.M. Goldberg, Mesenchymal cell-based repair of large, full-thickness defects of articular cartilage, J. Bone Joint Surg. Am. 76 (1994) 579–592.
[17] S.P. Bruder, A.A. Kurth, M. Shea, W.C. Hayes, N. Jaiswal, S. Kadiyala, Bone regeneration by implantation of purified, culture-expanded human mesenchymal stem cells, J. Orthop. Res. 16 (1998) 155–162.
[18] R.G. Young, D.L. Butler, W. Weber, A.I. Caplan, S.L. Gordon, D.J. Fink, Use of mesenchymal stem cells in a collagen matrix for Achilles tendon repair, J. Orthop. Res. 16 (1998) 406–413.
[19] C.J. Walsh, D. Goodman, A.I. Caplan, V.M. Goldberg, Meniscus regeneration in a rabbit partial meniscectomy model, Tissue Eng. 5 (1999) 327–337.
[20] O.N. Koc, S.L. Gerson, B.W. Cooper, S.M. Dyhouse, S.E. Haynesworth, A.I. Caplan, H.M. Lazarus, Rapid hematopoietic recovery after coinfusion of autologous-blood stem cells and culture-expanded marrow mesenchymal stem cells in advanced breast cancer patients receiving high-dose chemotherapy, J. Clin. Oncol. 18 (2000) 307–316.
[21] E.M. Horwitz, D.J. Prockop, L.A. Fitzpatrick, W.W. Koo, P.L. Gordon, M. Neel, M. Sussman, P. Orchard, J.C. Marx, R.E. Pyeritz, M.K. Brenner, Transplantability and therapeutic effects of bone marrow-derived mesenchymal cells in children with osteogenesis imperfecta, Nat. Med. 5 (1999) 309–313.
[22] K. Maruyama, S. Sugano, Oligo-capping: a simple method to replace the cap structure of eukaryotic mRNAs with oligoribonucleotides, Gene 138 (1994) 171–174.
[23] M. Sano, A. Umezawa, H. Abe, A. Akatsuka, S. Nonaka, H. Shimizu, M. Fukuma, J. Hata, EAT/mcl-1 expression in the human embryonal carcinoma cells undergoing differentiation or apoptosis, Exp. Cell Res. 266 (2001) 114–125.
[24] I. Sekiya, C.D. Colter, J.D. Prockop, BMP-6 enhances chondrogenesis in a subpopulation of human marrow stromal cells, Biochem. Biophys. Res. Commun. 284 (2001) 411–418.
[25] F. Barry, R.E. Boynton, B. Liu, J.M. Murphy, Chondrogenic differentiation of mesenchymal stem cells from bone marrow: differentiation-dependent gene expression of matrix components, Exp. Cell Res. 268 (2001) 189–200.
[26] Y. Suzuki, K. Yoshitomo-Nakagawa, K. Maruyama, A. Suyama, S. Sugano, Construction and characterization of a full length-enriched and a 5′-end-enriched cDNA library, Gene 200 (1997) 149–156.
[27] R.K. Naviaux, E. Costanzi, M. Haas, I.M. Verma, The pCL vector system: rapid production of helper-free, high-titer, recombinant retroviruses, J. Virol. 70 (1996) 5701–5705.
[28] T. Kiyono, S.A. Foster, J.I. Koop, J.K. McDougall, D.A. Galloway, A.J. Klingelhutz, Both Rb/p16INK4a inactivation and telomerase activity are required to immortalize human epithelial cells, Nature 396 (1998) 84–88.
[29] A. Hiraiwa, T. Kiyono, K. Segawa, K.R. Utsumi, M. Ohashi, M. Ishibashi, Comparative study on E6 and E7 genes of some cutaneous and genital papillomaviruses of human origin for their ability to transform 3Y1 cells, Virology 192 (1993) 102–111.
[30] C.D. Oh, S.H. Chang, Y.M. Yoon, S.J. Lee, Y.S. Lee, S.S. Kang, J.S. Chun, Opposing role of mitogen-activated protein kinase subtypes, erk-1/2 and p38, in the regulation of chondrogenesis of mesenchymes, J. Biol. Chem. 275 (2000) 5613–5619.
[31] M. Reyes, T. Lund, T. Lenvik, D. Aguiar, L. Koodie, C.M. Verfaillie, Purification and ex vivo expansion of postnatal human marrow mesodermal progenitor cells, Blood 98 (2001) 2615–2625.
[32] H.T. Yudate, M. Suwa, R. Irie, H. Matsui, T. Nishikawa, Y. Nakamura, D. Yamaguchi, Z.Z. Peng, T. Yamamoto, K. Nagai, K. Hayashi, T. Otsuki, T. Sugiyama, T. Ota, Y. Suzuki, S. Sugano, T. Isogai, Y. Masuho, HUNT: launch of a full-length cDNA database from the Helix Research Institute, Nucleic Acids Res. 29 (2001) 185–188.
[33] K. Matsubara, K. Okubo, Recent progress in human molecular biology and expression profiling of active genes in the body, Jpn. J. Pharmacol. 69 (1995) 181–185.
[34] M.S. Ko, J.R. Kitchen, X. Wang, T.A. Threat, A. Hasegawa, T. Sun, M.J. Grahovac, G.J. Kargul, M.K. Lim, Y. Cui, Y. Sano, T. Tanaka, Y. Liang, S. Mason, P.D. Paonessa, A.D. Sauls, G.E. DePalma, R. Sharara, L.B. Rowe, J. Eppig, C. Morrell, H. Doi, Large-scale cDNA analysis reveals phased gene expression patterns during preimplantation mouse development, Development 127 (2000) 1737–1749.
[35] L. Jia, M.F. Young, J. Powell, L. Yang, N.C. Ho, R. Hotchkiss, P.G. Robey, C.A. Francomano, Gene expression profile of human bone marrow stromal cells: high-throughput expressed sequence tag sequencing analysis, Genomics 79 (2002) 7–17.
[36] J. Cavallius, S.I. Rattan, B.F. Clark, Changes in activity and amount of active elongation factor 1 alpha in aging and immortal human fibroblast cultures, Exp. Gerontol. 21 (1986) 149–157.
[37] T. Giordano, D. Kleinsek, D.N. Foster, Increase in abundance of a transcript hybridizing to elongation factor I alpha during cellular senescence and quiescence, Exp. Gerontol. 24 (1989) 501–513.
[38] D. Pennica, T.A. Swanson, J.W. Welsh, M.A. Roy, D.A. Lawrence, J. Lee, J. Brush, L.A. Taneyhill, B. Deuel, M. Lew, C. Watanabe, R.L. Cohen, M.F. Melhem, G.G. Finley, P. Quirke, A.D. Goddard, K.J. Hillan, A.L. Gurney, D. Botstein, A.J. Levine, WISP genes are members of the connective tissue growth factor family that are up-regulated in wnt-1-transformed cells and aberrantly expressed in human colon tumors, Proc. Natl. Acad. Sci. USA 95 (1998) 14717–14722.
[39] P.W. Finch, J.S. Rubin, T. Miki, D. Ron, S.A. Aaronson, Human KGF is FGF-related with properties of a paracrine effector of epithelial cell growth, Science 245 (1989) 752–755.
[40] D.R. Hsu, A.N. Economides, X. Wang, P.M. Eimon, R.M. Harland, The Xenopus dorsalizing factor Gremlin identifies a novel family of secreted proteins that antagonize BMP activities, Mol. Cell. 1 (1998) 673–683.
[41] A. Zuniga, A.P. Haramis, A.P. McMahon, R. Zeller, Signal relay by BMP antagonism controls the SHH/FGF4 feedback loop in vertebrate limb buds, Nature 401 (1999) 598–602.
[42] C. Shukunami, C. Shigeno, T. Atsumi, K. Ishizeki, F. Suzuki, Y. Hiraki, Chondrogenic differentiation of clonal mouse embryonic cell line ATDC5 in vitro: differentiation-dependent gene expression of parathyroid hormone (PTH)/PTH-related peptide receptor, J. Cell Biol. 133 (1996) 457–468.
[43] T. Okamoto, T. Aoyama, K. Nishijo, T. Nakamata, T. Hosaka, T. Nakayama, T. Nakamura, T. Kiyono, J. Toguchida, Clonal heterogeneity in differentiation potential of immortalized human mesenchymal stem cells, Biochem. Biophys. Res. Commun. 295 (2002) 354–61.

ACADEMIC PRESS

Available online at www.sciencedirect.com

SCIENCE DIRECT®

Experimental Cell Research 288 (2003) 51–59

Experimental Cell Research

www.elsevier.com/locate/yexcr

In vivo cardiovasculogenesis by direct injection of isolated adult mesenchymal stem cells

Satoshi Gojo,[a,b] Noriko Gojo,[b] Yukiji Takeda,[a,c] Taisuke Mori,[a,c] Hitoshi Abe,[c] Shunei Kyo,[b] Jun-ichi Hata,[a,c] and Akihiro Umezawa[a,c,*]

[a] *National Research Institute for Child Health and Development, Tokyo, Japan*
[b] *Department of Cardiovascular Surgery, Saitama Medical Center, Saitama, Japan*
[c] *Department of Pathology, Keio University School of Medicine, Tokyo, Japan*

Received 12 December 2002

Abstract

The characterization of mesenchymal stem cells (MSCs) is of biological and clinical interest. We demonstrate that isolated MSCs, defined by $CD34^{low}$ c-kit^{+} $CD140a^{+}$ Sca-1^{high}, are able to differentiate into cardiomyocytes, endothelial cells, and pericytes or smooth muscle cells by direct injection into adult heart. In skeletal muscle and lung, they also contributed to formation of the vasculature. MSCs did not transform into malignant cells or form excess extracellular matrix. This study suggests that MSCs may supply an ideal donor source of cardiovascular cells in patients with cardiopulmonary diseases.

Keywords: Regeneration; Transplantation; Cell therapy; Cardiomyocyte; Marrow stroma

Introduction

The existence of stem cells for nonhematopoietic cells in bone marrow was first suggested by Cohnheim [1] about 130 years ago. Recently, it was reported that marrow-derived mesenchymal stem cells (MSCs) differentiate into most somatic cells including osteoblasts, chondrocytes, myoblasts, and adipocytes such as adult neural stem cells [2] when placed in appropriate in vitro [3,4] and in vivo environments [5] or injected into blastocysts [6]. We have shown that stromal cells are able to generate cardiomyocytes in vitro [7,8]. However, most of these experiments were performed with heterogeneous stromal cells that had been obtained by adherence to plastic culture dishes [9]. Since it was demonstrated that bone marrow-derived stromal cells were purified to a homogeneous population that met the criteria for nonhematopoietic stem cells [10], these cells have been termed mesenchymal stem cells because they generate an array of cells, defined as mesenchymal cells.

Major advances have been made in the prevention, diagnosis, and treatment of cardiovascular diseases. However, morbidity and mortality from cardiovascular diseases continue to be an enormous burden experienced by many individuals with substantial economic cost. Recently, it was reported that adult bone marrow-derived cells can be reprogrammed to differentiate into various cell types, including liver cells [11], and neuronal-type cells [12] in vivo. In this study, our results present two novel findings in marrow-derived MSCs, i.e., the presence of a set of surface marker proteins and site-specific differentiation into cardiovascular cells in adult.

Materials and methods

Cell culture

Bone marrow-derived stromal cells were cultured by using methods previously described [4]. Bone marrow cells

* Corresponding author. Department of Pathology, Keio University School of Medicine, 35 Shinanomachi, Shinjuku-ku, Tokyo 160-8582, Japan. Fax: +81-3-3353-3290.
E-mail address: umezawa@1985.jukuin.keio.ac.jp (A. Umezawa).

0014-4827/03/$ – see front matter
doi:10.1016/S0014-4827(03)00132-0

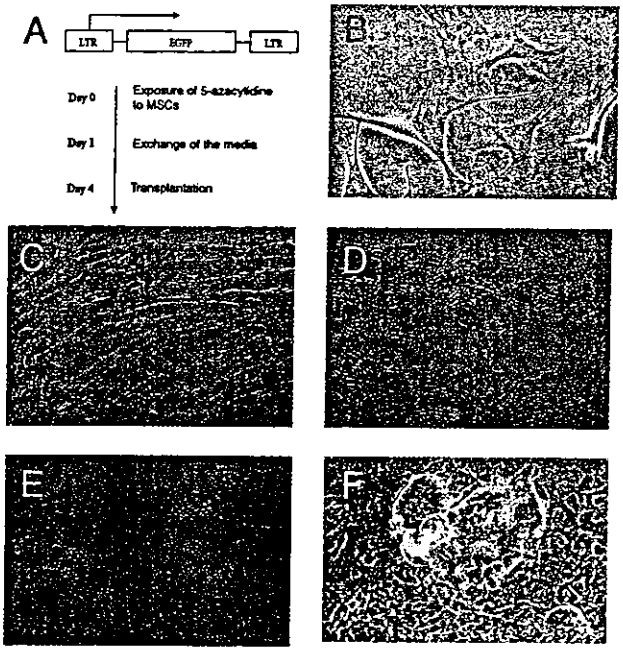

1

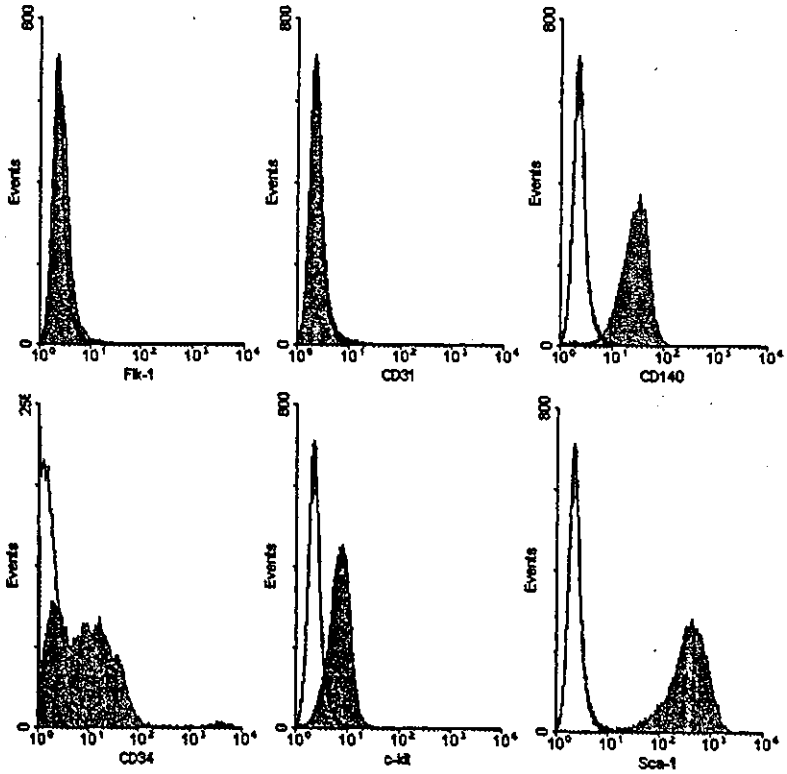

Surface Marker	Expression	Surface Marker	Expression	Surface Marker	Expression
Flk-1	-	CD14	-	CD54	-
CD31	-	CD29	++	CD90	-
CD144	+	CD41	+	CD102	-
CD34	+	CD44	+++	CD105	-
c-kit	+	CD45	-	CD106	-
Sca-1	+++	CD49b	-	Ly-6c	++
CD140	++	CD49d	-	Ly-6g	-

2

were obtained from female C3H/HeJ mice. Cells were cultured in Iscove's modified Dulbecco's medium (IMDM) supplemented with 20% fetal bovine serum and penicillin (100 μg/ml)/streptomycin (250 ng/ml)/amphotericin B (85 μg/ml) at 33°C in humid air with 5% CO_2. After a series of passages, attached marrow stromal cells became homogeneous and were devoid of hematopoietic cells. Immortalized cells were obtained by frequent subculture for more than 4 months. To induce demethylation of genomic DNA, cells were treated with 3 μmol/l of 5-azacytidine (Sigma Chemical Co., St. Louis, MO, USA) for 24 h.

A number of clones were isolated by limiting dilution. Subcloned cells were maintained and again exposed to 5-azacytidine for 24 h. We selected a unique population of immortalized cells that expressed the hematopoietic stem markers $CD34^{low/-}$ and $c\text{-}kit^{+}$ and the mesenchymal marker $CD140a^{+}$ for subsequent experiments, because this cell population is believed to be one of the most upstream progenitors among our isolated cell population. The retroviral vector used in this study contains enhanced green fluorescent protein (EGFP) driven by the long terminal repeat enhancer/promoter of the Moloney murine leukemia virus. The ecotropic virus-producing GP + E86 cells were created as a packaging cell. Supernatants from the vector-producing cells, with a titer of 5×10^5 particles per milliliter, were used to transduce MSCs. Gene transduction was performed by three exchanges of the culture media of MSCs plated at density of 1×10^5 cells per 10 cm of tissue culture dish with the supernatant of the retroviral supernatant over 72 h with polybrene. Following transduction of the EGFP gene, the cells were maintained and used as donor cells in subsequent experiments. The transduction efficiency was determined by fluorescence-activating cell sorting (FACS) analysis.

FACS analysis

All samples were treated by water lysis to delete red blood cells. Cells were incubated with 0.01 μg/μl monoclonal antibody in Hanks' balanced salt solution (containing 0.1% albumin and 0.1% sodium azide) per 1×10^6 cells. When the first antibody was conjugated with biotin, cells were then washed twice and incubated with 1 μg of streptoavidin-phycoerythrin (GibcoBRL, Gaithersburg, MD, USA) for 30 min on ice. Purified antibodies in the first step were stained with 1 μg of fluorescein isothiocyanate-conjugated goat anti-mouse antibody. Controls included cells stained with individual isotypes (mouse IgG_1 or rat IgG_{2a}). Incubation was performed in the presence of 10 μg of mouse immunoglobulin to prevent nonspecific antibody binding. Anti-mouse Flk-1 (KDR or VEGF-receptor 2), CD31 (PECAM-1), CD34, c-kit, Sca-1 (Ly-6A/E), CD140a, CD144 (VE-Cadherin; endothelial cell-specific marker), CD14 (a marker for macrophages and dendritic cells), CD29 (integrin β1), CD41 (integrin αIIβ chain), CD44 (Pgp-1/Ly-24), CD45 (leukocyte common antigen), CD49b (integrin α2 chain), CD49d (integrin α4 chain), CD54 (ICAM-1), CD90 (Thy-1), CD102 (ICAM-2), CD105 (Endoglin), CD106 (VCAM-1), Ly-6C, Ly-6G (Gr-1), and isotype control antibodies were purchased from Pharmingen Pharmaceutical, Inc. (San Diego, CA, USA). Dead cells were removed by washing twice with Hanks' balanced salt solution, then propidium iodide was added to each test tube at a concentration of 1 μg/ml just before acquisition by FACScan flow cytometry (Becton Dickinson, Bedford, MA, USA) with the argon laser at 488 nm. List mode data for 30,000 to 50,000 cells were collected in the propidium iodide gate.

Cellular transplantation

Following priming by 5-azacytidine, the cells were cultured for an additional 3 days (Fig. 1A). Then these cells were harvested with 0.05% trypsin and 0.25 mM EDTA and suspended as single cells at a concentration of 1×10^5 cells/μl with phosphate-buffered saline (PBS). Cell viability in suspension, determined by 0.05% erythrosine dye exclusion, was 90% to 95%. After general anesthesia of the recipient mice by an intraperitoneal injection of pentobarbiturate 0.05 mg/g body weight, a transverse incision was made under the arch of a rib. The xiphoid process was inverted to the head, and the liver was pushed inferiorly so that the heart became visible through the diaphragm. Immediately before implantation, the cell suspension was drawn up into a 50-μl Hamilton syringe with a 31-gauge needle. A 10-μl portion of the cell suspension was injected into the ventricular myocardium or the inferior vena cava of syngeneic adult recipient mouse (C3H/HeJ, purchased from Clea Japan, Inc., Tokyo, Japan), aged 8 to 10 weeks [13]. Cell transplantations were also performed into the quadrant

Fig. 1. In vitro characteristics of the mesenchymal stem cells (MSCs) as a pluripotent stem cell model. (A) Construction of the recombinant retrovirus carrying enhanced green fluorescent protein (EGFP) cDNA and experimental procedure of cell transplantation. (B) Phase-contrast micrograph of isolated MSCs at the semiconfluent stage. (C–F) In vitro differentiation of the isolated MSCs. (C) Cell clusters spontaneously beat with the characteristic findings specific to cardiomyocytes such as branched structure. (D) Myotubes with multinuclei do not spontaneously beat. (E) Clusters of adipocytes. (F) Bone matrix produced by the cells.

Fig. 2. Flow cytometric analysis of cell surface markers in murine mesenchymal stem cells (MSCs). Endothelial cell markers Flk-1 and CD31 are negative. Mesenchymal marker CD140a and hematopoietic cell markers c-kits and Sca-1 are positive. Although CD34 expression has two peaks, negative and low positive at the periods of the transplantation, the more $CD34^{low}$ cells are generated the longer cultivation after the exposure to 5-azacytidine. Further phenotypic analysis was shown in the table (details in the supplements). The stainings of MSCs were performed according to Pharmingen protocols. All the antibodies used were from Pharmingen.

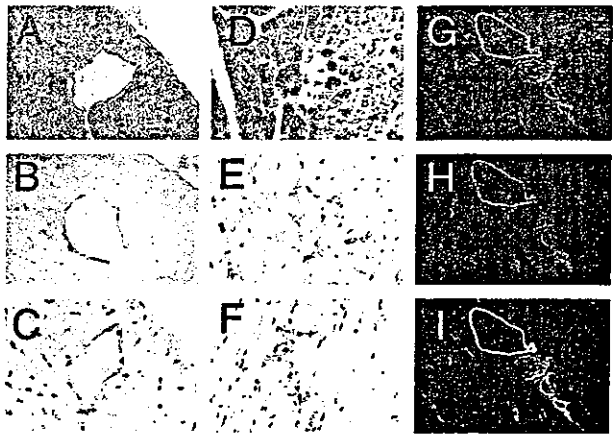

3

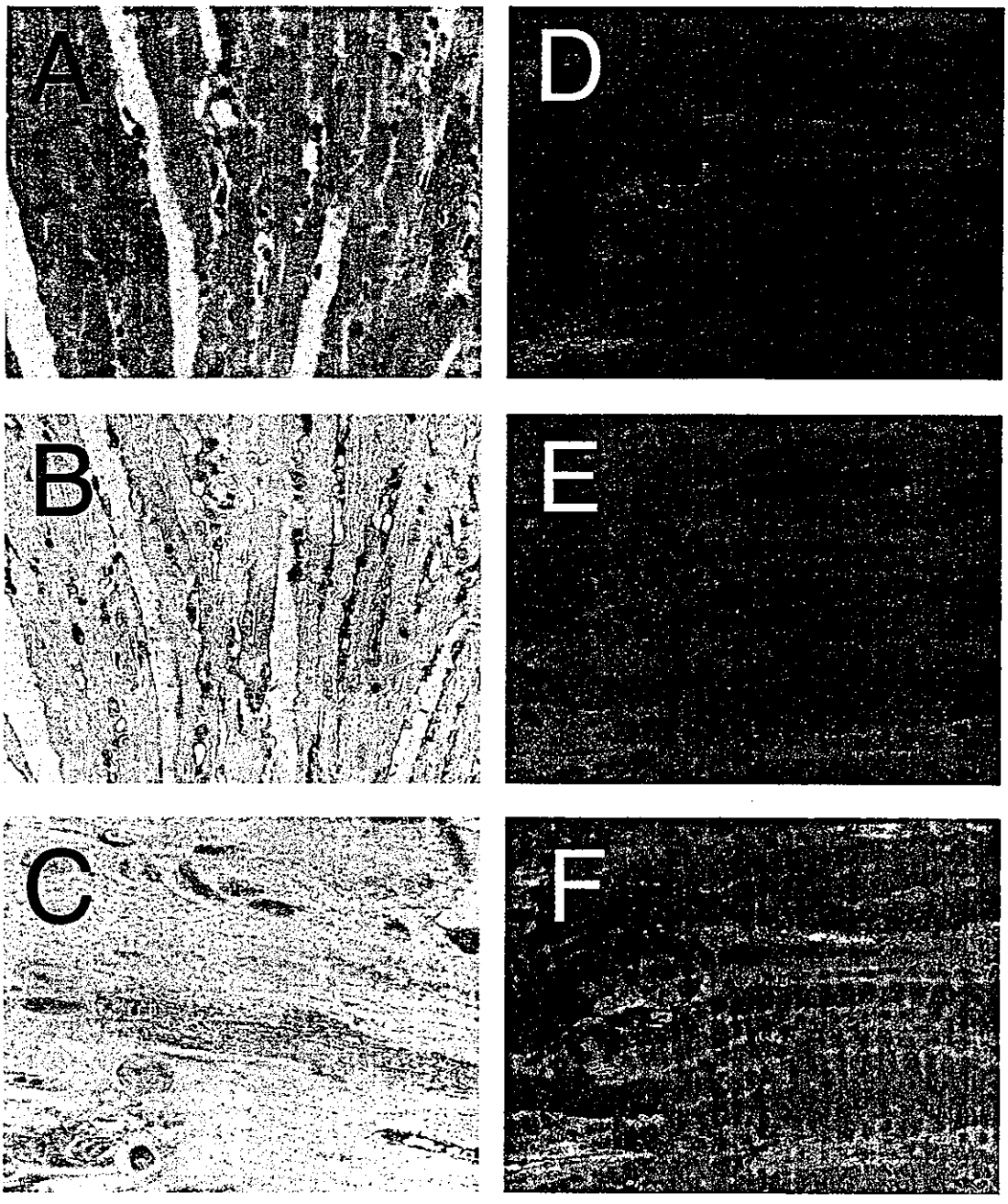

4

muscles at a dose of 1×10^6 and 1×10^8 cells per each mouse. At 1, 4, 8, and 12 weeks after the transplantation, three to five mice were killed, and the lung, heart, thymus, liver, spleen, kidney, stomach, small intestine, colon, and brain were harvested from each animal. All animals received humane care in compliance with the *Principles of Laboratory Animal Care,* formulated by the National Society for Medical Research, and the *Guide for the Care and Use of Laboratory Animals,* prepared by the Institute of Laboratory Animal Resources and published by the National Institutes of Health (NIH Publication No. 86-23, revised 1985). All mice were maintained in a laminar-flow rack in our animal facility.

Histological analyses

Tissues were fixed in 10% neutral buffered formalin and embedded in paraffin. Tissue sections (6 μm) were mounted on poly-L-lysine-coated slides. After deparaffinization with xylene, tissues were rinsed in acetone or ethanol. Slides were incubated in 0.3% H_2O_2 in methanol for 30 min. After washing in PBS, tissues were preblocked for 30 min with 5% normal swine serum. They were incubated overnight at 4°C with mouse monoclonal antibody against recombinant green fluorescent protein (Clontech Laboratories, Inc., Palo Alto, CA, USA, catalogue no. 8362-1) at 1:500. After rinsing in PBS, slides were incubated with horseradish peroxidase-conjugated swine anti-mouse immunoglobulin diluted at 1:100 with 1% bovine serum albumin (BSA) in PBS, and washed in cold PBS. Staining was developed by using a solution containing diaminobenzidine and 0.01% H_2O_2 in 0.05 M Tris-HCl buffer, pH 6.7. Slides were counterstained with methylgreen or hematoxylin. Harvested organs were fixed in 10% formaldehyde and stained with hematoxylin and eosin, or anti-EGFP. Slices with positive signals for EGFP were further stained with anti-CD31 (PECAM-1) (M-20, Santa Cruz Biotechnology, Inc., Santa Cruz, CA, USA). The total numbers of EGFP-positive cells per section were counted.

Frozen sections (6 μm) of the samples were used to detect the donor cells and the differentiation status by using alkaline phosphatase and fluorescence. After fixation with acetone and the blocking with PBS containing 5% rabbit serum, anti-GFP antibody was overlaid at 4°C overnight. Following three washes with PBS, the slides were incubated with anti-mouse IgG antibody conjugated with alkaline phosphatase for 1 h at room temperature. Visualization was achieved through the alkaline phosphatase detection system. In the case of fluorescence, anti-CD31 or anti-desmin (Bio-Science Products AG, Emmenbrücke, Switzerland) was used for first antibody, and rat anti-mouse IgG antibody conjugated with tetramethylrhodamine isothiocyanate (T4280, Sigma) or goat anti-mouse IgG antibody conjugated with rhodamine (M116, Leinco Technology, Inc., St. Louis, MO, USA) was used for second antibody, respectively.

Results

Gene transduction

Following retrovirus-mediated gene transduction of isolated MSCs derived from marrow stroma with the EGFP gene and subsequent culture (Fig. 1A and B), the cells were evaluated by FACS analysis and confocal laser microscopy. After three 24-h exposures of the cells to the retroviral vector, 70% to 80% of the cells expressed the reporter EGFP gene. The isolated MSCs retained the ability to generate cardiomyocytes, skeletal muscle cells, adipocytes, and osteoblasts in vitro (Fig. 1C–F).

Surface analysis of mesenchymal stem cell line

A true mesenchymal stem marker has yet to be identified. The putative MSCs ($CD34^{low/-}$ c-kit^+ $CD140a^+$), used in this experiment, expressed CD34 on the fourth day after the 5-azacytidine treatment (Fig. 2). Sca-1, CD29, and CD44 were expressed in all mesenchymal cell lines examined at moderate to high levels. Further surface analysis showed that these cells also expressed CD41, CD144, and Ly-6C. The cells were negative for Flk-1, CD31, CD14, CD45, CD49b, CD49d, CD54, CD90, CD102, CD105, CD106, and Ly-6G. It was previously reported that human mesenchymal stem cells were successfully isolated and could differentiate into osteocytes, chondrocytes, and adipocytes [14]. Our surface antigens analyses showed the differences from those on human MSCs, which express CD105 but not CD34.

Fig. 3. Generation of endothelial cells by the isolated mesenchymal stem cells (MSCs). The MSCs expressing enhanced green fluorescent protein (EGFP) were directly injected into the heart, and were histologically analyzed in the heart 1 week (A–C) or 3 months (D–F) after the grafting ($n = 41$). Sections for donor-derived cells were stained with hematoxylin and eosin (A and D), anti-EGFP antibody (B and E), or anti-CD31 antibody (C and F) by peroxidase method. CD31 staining demonstrates that the donor MSCs differentiated into the endothelial cells. The vessels contained red blood cells (D), suggesting that the vessels connected to the host vascular system and supplied blood to the tissues. The merge (I) of green fluorescence of injected MSCs (G) and rhodamine of CD31 (H) clearly demonstrated that the MSCs differentiated into the endothelium.

Fig. 4. Differentiation of the isolated mesenchymal stem cells (MSCs) into cardiomyocytes. Enhanced green fluorescent protein (EGFP)-labeled MSCs could be recognized morphologically as the cardiomyocytes in the heart 3 months after transplantation (A, hemotoxglin and eosin staining; B and C, peroxidase staining). The EGFP-positive donor cells exhibit cardiomyocyte-specific features such as a single nucleus in the middle of the cells, branching, striation, and intercalated disks. The injected donor cells labeled with EGFP were also detected by green fluorescence. (D) Green fluorescence of EGFP-labeled donor cells. (E) Immunohistochemistry against desmin (red). (F) Merge.

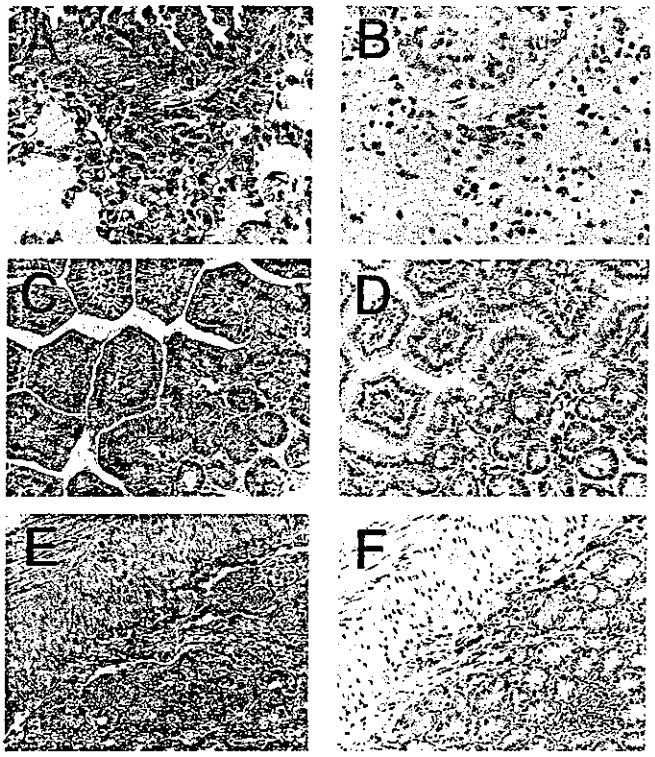

Fig. 5. Donor cell distribution after intravenous injection of the mesenchymal stem cells (MSCs) expressing enhanced green fluorescent protein (EGFP). EGFP immunoreactivities were detected in the lung (A and B), the small intestine (C and D), and the stomach (E and F). Recipient tissues (n = 28) were examined at 3 months after the transplantation of MSCs.

Engraftment of mesenchymal stem cells

Cells, which were grafted into the heart, generated neoangiogenesis near the injection site within 1 week after transplantation. The number of vessels increased significantly in the injection region and EGFP-positive donor cells could be identified in these vessels (Fig. 3A and B). Immunohistochemistry with anti-CD31, a marker for endothelium, confirmed that the donor cells of the newly formed vessels had differentiated into endothelium (Fig. 3C). At 3 months after transplantation into the heart, the donor-derived endothelium that formed vessels were observed in in vivo environments (Fig. 3D–F).

Furthermore, we assessed the fluorescence conjugated to the anti-CD31 antibody. Double-positive cells for GFP and CD31 were clearly demonstrated in the injection area (Fig. 3G–I). Donor cells engrafted in the heart appeared to maintain the characteristics of stem cells, which continue to provide the progenies, i.e., differentiated endothelial cells, in this case. At this time point, cardiomyocytes expressing EGFP protein were present in juxtapositions of both donor to donor and donor to host cells in the heart around the injection area (Fig. 4A–C). These cells formed striated muscles with a branched structure, which distinguished them from skeletal muscle cells. Another cardiac muscle-specific finding, an intercalated disk, was found at the longitudinal end of donor cells. Moreover, the alignment of the implanted cells observed in this study was parallel to the host cardiomyocytes, suggesting that the donor cells possibly cooperate with cardiac contraction. We reconfirm the presence of donor cells by visualization with alkaline phosphatase as well as with EGFP. Positive signals for alkaline phosphatase (data not shown) and the green fluorescence were clearly recognized in the injected donor cells (Fig. 4D–F).

Quantification of the EGFP-positive MSCs from serial sections showed that an estimated 2,500 donor cells were viable in the ventricle 1 week after grafting 1×10^6 cells (0.25%) into the heart. The number of endothelial cells and cardiomyocytes originating from the injected cells were 1,625 and 75 cells, respectively. The remaining donor cells could not be characterized using immunohistochemistry. The number of donor-derived cells in the heart 3 months after transplantation decreased to 1,100 cells, including 275 endothelial cells and 25 cardiomyocytes.

We injected mesenchymal stem cells intravenously to clarify whether vasculogenesis could occur elsewhere, especially in the lung. At 1 week after intravenous injection,

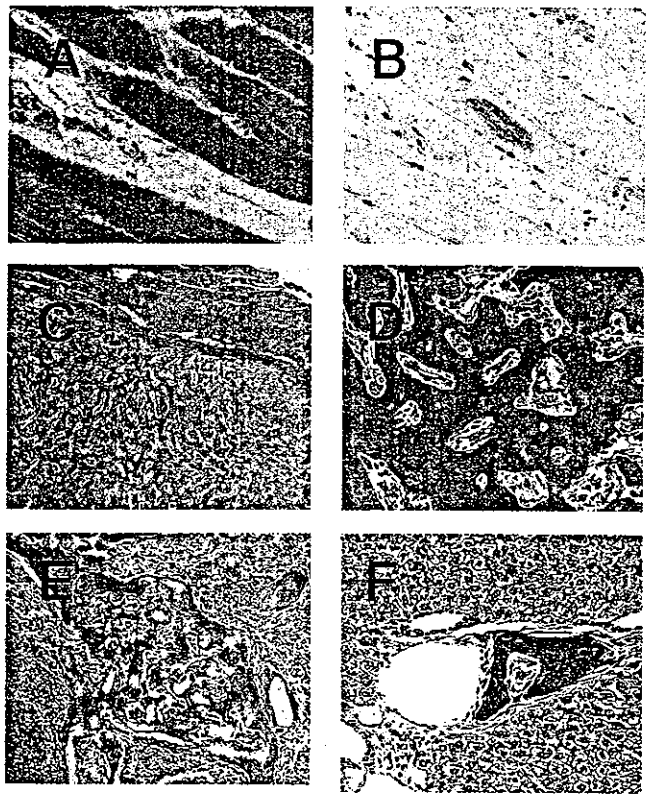

Fig. 6. Generation of endothelium and skeletal muscle by the mesenchymal stem cells (MSCs). The MSCs also differentiated into the skeletal muscle cells and fused to the host skeletal muscle 3 months after the grafting (A and B). Bone formation was detected in the skeletal muscle after a megadose injection of the cells (C and D). Similarly, osteogenesis was seen in the spleen (E) and the liver (F) 2 months after the injection of the MSCs into the spleen. Bone formation in the liver is probably due to transfer of donor cells via portal vein from the spleen to the liver.

mice showed predominant targeting of donor cells to the lung, where clusters of donor cells were seen in lymphatic vessels and in the vessel walls. At 4 weeks following transplantation, very few cell clusters remained, and some EGFP-positive cells covered the vessel lumens completely (Fig. 5A and B). Although EGFP-positive cells in the lung were negative for the vascular endothelium marker anti-CD31 at 1 week, they had formed tube-like structures 4 weeks after intravenous injection, suggesting that they had differentiated into smooth muscle cells or pericytes. Only a small portion of stromal cells in the interstitial space of the lung expressed EGFP 12 weeks after the grafting (Fig. 5C and D). No obvious tissue-specific differentiation was observed. In addition, no tumorous growth was seen in any tissue throughout the experiment.

Small numbers of EGFP-positive cells were also seen in the brain, thymus, uterus, and kidney throughout these experiments (data not shown). Although few EGFP-positive cells were present in the stomach and small intestine in the early phase after both intravenous and intramuscular transplantation, many donor cells were recognized in these organs at 12 weeks following injection (Fig. 5E and F).

We examined the dose escalation of MSC injection in the skeletal muscle. Donor mesenchymal stem cells differentiated along a similar time course into endothelial cells and myocytes in skeletal muscle as in heart. By 1 week after implantation, the donor cells had differentiated into endothelial cells and formed vessels in the graft sites. A skeletal myocyte phenotype was first observed in cells derived from the donor cells at 3 months after transplantation (Fig. 6A and B). When a megadose of cells (1×10^8 cells/mouse) was implanted into one site in skeletal muscles, no endothelial cells or skeletal myocytes emerged at any observation time point. However, we detected a massive hard mass in the thigh, and hematoxylin and eosin staining indicated that the mass was newly formed bone (Fig. 6C and D). Transplantation into the spleen also led to bone formation in the spleen and liver (Fig. 6E and F).

Discussion

This experiment demonstrated that MSCs retain their plasticity in the adult body in addition to being able to differentiate into mesoderm-derived cells in the fetus [15]. Immortalized cells, including MSCs, have specific patterns of DNA methylation, and because the established methylation pattern is subsequently maintained with considerable fidelity [16–18], the cell phenotype remains in its original state in the immortalized cells. The silenced genes are stably inherited throughout the culture period, and such genes can be demethylated and reactivated by a demethylating agent [19]. 5-Azacytidine, a cytosine analog, has a remarkable effect on transdifferentiation of cells and has been shown to induce differentiation of mesenchymal cells into cardiomyocytes, skeletal myocytes, adipocytes, and chondrocytes [7,20].

5-Azacytidine is incorporated into DNA and has been shown to cause extensive demethylation. The demethylation is attributable to covalent binding of DNA methyltransferase to 5-azacytidine in the DNA [21], with the subsequent reduction of enzyme activity in cells resulting in dilution out and loss of methylation at many sites in the genome. This may in turn account for reactivation of cardiomyogenic "master gene(s)," such as MEF-2C, GATA4, dHAND, TEF-1 and Nkx2.5/Csx, by 5-azacytidine, leading to transdifferentiation of MSCs into cardiomyocytes.

Isolated adult MSCs could differentiate into the progeny in a tissue-specific manner according to their ultimate destination. Nonphysiological cells, such as osteocytes, chondrocytes, or adipocytes, were not generated in this experimental setting in 41 transplants, despite that these donor cells have the potential to generate a variety of mesoderm-derived cells in vitro. Although there were some EGFP-positive cells in the interstitial spaces, no newly formed matrices were observed. There was no significant inflammatory reaction, consistent with the long survival of these donor stem cells in the heart. In this transplant procedure into the heart that we have been performing since 1992, no lethal arrhythmia has ever been recorded [13].

It has been generally accepted that cardiac myocytes are unable to divide once cell proliferation ceases shortly after birth in the mammalian heart, because mitotic figures have not been detected in myocytes [22]. Although genetically altered cardiomyocytes induced DNA synthesis in vivo and in vitro [23,24], it remained unclear whether normal or diseased cardiac myocytes can synthesize DNA. Adult hearts often exhibit a polypoid structure, which results from stochastic accumulation of mutations as cells pass through cell cycle check points [25]. However, the hypothesis that the life span of terminally differentiated cells corresponds to that of the body may contradict the concept of cellular aging. Recently, there are a number of lines of evidence that suggest that there is some cell proliferation in the adult heart. A mitotic index was calculated in patients with heart failure and 11 myocyte nuclei per 1 million cells exhibited mitotic images [26], and karyokinesis and cytokinesis were observed by confocal microscopy in adult normal subjects and patients with dilated cardiomyopathy [27]. Our data together with a report [28] that bone marrow-derived cells provided cardiomyocytes and skeletal muscle in dystrophic mdx mice support this hypothesis.

The potential for engraftment of bone marrow-derived stromal cells following transplantation has been debated in mice [29] and humans [30]. Since stromal cells are estimated to account for only around 1% of total nucleated marrow cells [31], it is very difficult to monitor engraftment of stromal cells in bone marrow transplantation. But, transplantation of a portion enriched for stromal cells from crude human bone marrow showed engraftment into SCID mice. Murine mesenchymal cells were distributed in the lung,

spleen, cartilage, and bone marrow up to 5 months after infusion into irradiated mice [32]. Taken together with our results, these data suggest that a significant number of stromal cells can be expected to engraft and survive in various organs.

We previously observed the fate of bone produced by immortalized osteoblasts, and found that the ectopically generated bone keeps its size and shape for 12 months [33]. Furthermore, the transplanted cells did not metastasize like tumor cells. In this study, the MSC-derived cardiomyocytes remained unchanged for at least 8 weeks. Although injected cells did not escape from the transplanted sites or settle in other organs for at least 8 weeks, long-term observation is necessary to confirm the survival of the differentiated cells and rule out the possibility of transformation.

In this model, we could not confirm whether the donor cells enforced the recipient heart. Crude bone marrow cells, skeletal myocytes, or smooth muscle cells grafted into an infarcted area are able to improve its elasticity, but not contractility [34]. Transplantation of fetal or neonatal cardiomyocytes has been demonstrated to connect the graft cells and the host cardiomyocytes [35] and improve cardiac function, including contractility [36]. Taken together with these studies, the existence of autologous cardiomyocytes or the precursors for the transplantation should be only one prerequisite for a clinical cell therapy for cardiac diseases. When compared with hematopoietic stem cells, our mesenchymal stem cells were easily propagated [4], and sufficient numbers of cells for a clinical application can be obtained in vitro.

The present study demonstrates that when the isolated adult MSCs are introduced into adult heart and lung, they can generate cardiovascular cells. When FACS sorting is set for this novel population, $CD34^{low}$ $c\text{-}kit^{+}$ $CD140a^{+}$ $Sca\text{-}1^{high}$, the fraction of human bone marrow cells will be highly enriched for cardiovascular cells.

Acknowledgments

We would like to express sincere thanks to K. Sakurada and Y. Yamada (Kyowa Hakko Kogyo Co., Ltd.), H. Imabayashi, A. Suzuki, and K. Fukuda for support throughout the work, and T. Inomata, Y. Setoyama, and N. Onoda for providing expert technical assistance.

References

[1] J. Cohnheim, Ueber Entzündung und Eiterung, Virchows Arch. 40 (1867) 1.
[2] D.L. Clarke, C.B. Johansson, J. Wilbertz, B. Veress, E. Nilsson, H. Karlstrom, U. Lendahl, J. Frisen, Generalized potential of adult neural stem cells, Science 288 (2000) 1660–1663.
[3] A. Umezawa, K. Tachibana, K. Harigaya, S. Kusakari, S. Kato, Y. Watanabe, T. Takano, Colony-stimulating factor 1 is downregulatd during the adipocyte differentiation of H-1/A marrow stromal cells and induced by cachectin/tumor necrosis factor, Mol. Cell. Biol. 11 (1991) 920–927.
[4] A. Umezawa, T. Maruyama, K. Segawa, R.K. Shadduck, A. Waheed, J. Hata, Multipotent marrow stromal cell line is able to induce hematopoiesis in vivo, J. Cell. Physiol. 151 (1992) 197–205.
[5] D.J. Prockop, Marrow stromal cells as stem cells for nonhematopoietic tissues, Science 276 (1997) 71–74.
[6] Y. Jiang, B.N. Jahagirdar, R.L. Reinhardt, R.E. Schwartz, C.D. Keene, X.R. Ortiz-Gonzalez, M. Reyes, T. Lenvik, T. Lund, M. Blackstad, J. Du, S. Aldrich, A. Lisberg, W.C. Low, D.A. Largaespada, C.M. Verfaillie, Pluripotency of mesenchymal stem cells derived from adult marrow. Nature 418 (2002) 41–49 .
[7] S. Makino, K. Fukuda, S. Miyoshi, F. Konishi, H. Kodama, H. Pan, J.M. Sano, T. Takahashi, S. Hori, H. Abe, J. Hata, A. Umezawa, A.S. Ogawa, Cardiomyocytes can be generated from marrow stromal cells in vitro, J. Clin. Invest. 103 (1999) 697–705.
[8] D. Hakuno, K. Fukuda, S. Makino, F. Konishi, Y. Tomita, T. Manabe, Y. Suzuki, A. Umezawa, S.. Ogawa, Bone marrow-derived regenerated cardiomyocytes (CMG cells) express functional adrenergic and muscarinic receptors, Circulation 105 (2002) 380–386.
[9] A.J. Friedenstein, J.F. Gorskaja, N.N. Kulagina, Fibroblast precursors in normal and irradiated mouse hematopoietic organs, Exp. Hematol. 4 (1976) 267–274.
[10] P.J. Simmons, B. Torok-Storb, Identification of stromal cell precursors in human bone marrow by a novel monoclonal antibody, STRO-1, Blood 78 (1991) 55–62.
[11] B.E. Petersen, W.C. Bowen, K.D. Patrene, W.M. Mars, A.K. Sullivan, N. Murase, S.S. Boggs, J.S. Greenberger, J.P. Goff, Bone marrow as a potential source of hepatic oval cells, Science 284 (1999) 1168–1170.
[12] J. Kohyama, H. Abe, T. Shimazaki, A. Koizumi, K. Nakashima, S. Gojo, T. Taga, H. Okano, J. Hata, A. Umezawa, Brain from bone: efficient "meta-differentiation" of marrow stroma-derived mature osteoblasts to neurons with Noggin or a demethylating agent, Differentiation 68 (2001) 235–244.
[13] S. Gojo, S. Kitamura, O. Hatano, A. Takakusu, K. Hashimoto, Y. Kanegae, I. Saito, Transplantation of genetically marked cardiac muscle cells, J. Thorac Cardiovasc. Surg. 113 (1997) 10–18.
[14] M.F. Pittenger, A.M. Mackay, S.C. Beck, R.K. Jaiswal, R. Douglas, J.D. Mosca, M.A. Moorman, D.W. Simonetti, S. Craig, D.R. Marshak, Multilineage potential of adult human mesenchymal stem cells, Science 284 (1999) 143–147.
[15] K.W. Liechty, T.C. MacKenzie, A.F. Shaaban, A. Radu, A.M. Moseley, R. Deans, D.R. Marshak, A.W. Flake, Human mesenchymal stem cells engraft and demonstrate site-specific differentiation after in utero transplantation in sheep, Nat. Med. 6 (2000) 1282–1286.
[16] S. Kochanek, M. Toth, A. Dehmel, D. Renz, W. Doerfler, Interindividual concordance of methylation profiles in human genes for tumor necrosis factors alpha and beta, Proc. Natl. Acad. Sci. USA 87 (1990) 8830–8834.
[17] A. Behn-Krappa, I. Holker, U. Sandaradura de Silva, Doerfler, W. Patterns of DNA methylation are indistinguishable in different individuals over a wide range of human DNA sequences, Genomics 11 (1991) 1–7.
[18] A. Umezawa, H. Yamamoto, K. Rhodes, M.J. Klemsz, R.A. Maki, R.G. Oshima, Methylation of an ETS site in the intron enhancer of the keratin 18 gene participates in tissue-specific repression, Mol. Cell. Biol. 17 (1997) 4885–4894.
[19] S.J. Compere, R.D. Palmiter, DNA methylation controls the inducibility of the mouse metallothionein I gene in lymphoid cells, Cell 25 (1981) 233–240.
[20] S. Taylor, P.A. Jones, Multiple new phenotypes induced in 10T1/2 cells and 3T3 cells treated with 5-azacytidine, Cell 17 (1979) 771–779.
[21] D.V. Santi, A. Norment, C.E. Garrett, Covalent bond formation between a DNA-cytosine methyl transferase and DNA containing 5-aza-cytidine, Proc. Natl. Acad. Sci. USA 81 (1984) 6993–6997.

[22] K.W. Karsner, O. Saphir, T.W. Todd, The state of the cardiac muscle in hypertrophy and atrophy, Am. J. Pathol. 1 (1925) 351–371.
[23] L.A. Kirshenbaum, M.D. Schneider, Adenovirus E1A represses cardiac gene transcription and reactivates DNA synthesis in ventricular myocytes, via alternative pocket protein- and p300-binding domains, J. Biol. Chem. 270 (1995) 7791–7794.
[24] M.H. Soonpaa, G.Y. Koh, L. Pajak, S. Jing, H. Wang, M.T. Franklin, K.K. Kim, L.J. Field, Cyclin D1 overexpression promotes cardiomyocyte DNA synthesis and multinucleation in transgenic mice, J. Clin. Invest. 99 (1997) 2644–2654.
[25] M.H. Soonpaa, L.J. Field, Survey of studies examining mammalian cardiomyocyte DNA synthesis, Circ. Res. 83 (1998) 15–26.
[26] F. Quaini, E. Cigola, C. Lagrasta, G. Saccani, E. Quaini, C. Rossi, G. Olivetti, P. Anversa, End-stage cardiac failure in humans is coupled with the induction of proliferating cell nuclear antigen and nuclear mitotic division in ventricular myocytes, Circ. Res. 75 (1994) 1050–1063.
[27] J. Kajstura, A. Leri, N. Finato, C. Di Loreto, C.A. Beltrami, P. Anversa, Myocyte proliferation in end-stage cardiac failure in humans, Proc. Natl. Acad. Sci. USA 95 (1998) 8801–8805.
[28] R.E. Bittner, C. Schofer, K. Weipoltshammer, S. Ivanova, B. Streubel, E. Hauser, M. Freilinger, H. Hoger, A. Elbe-Burger, F. Wachtler, Recruitment of bone-marrow-derived cells by skeletal and cardiac muscle in adult dystrophic mdx mice, Anat. Embryol. (Berl.) 199 (1999) 391–396.
[29] L. Ding, S. Lu, R. Batchu, R.S. Iii, N. Munshi, Bone marrow stromal cells as a vehicle for gene transfer, Gene Ther. 6 (1999) 1611–1616.
[30] P.J. Simmons, D. Przepiorka, E.D. Thomas, B. Torok-Storb, Host origin of marrow stromal cells following allogeneic bone marrow transplantation, Nature 328 (1987) 429–432.
[31] A. Keating, L. Berkahn, R. Filshie, A Phase I study of the transplantation of genetically marked autologous bone marrow stromal cells, Hum. Gene Ther. 9 (1998) 591–600.
[32] R.F. Pereira, K.W. Halford, M.D. O'Hara, D.B. Leeper, B.P. Sokolov, M.D. Pollard, O. Bagasra, D.J. Prockop, Cultured adherent cells from marrow can serve as long-lasting precursor cells for bone, cartilage, and lung in irradiated mice, Proc. Natl. Acad. Sci. USA 92 (1995) 4857–4861.
[33] K. Ochi, G. Chen, T. Ushida, S. Gojo, K. Segawa, H. Tai, K. Ueno, H. Ohkawa, T. Mori, A. Yamaguchi, Y. Toyama, J. Hata, A. Umezawa, Use of isolated mature osteoblasts in abundance acts as desired-shaped bone regeneration in combination with a modified poly-DL-lactic-co-glycolic acid (PLGA)-collagen sponge, J. Cell. Physiol. 194 (2003) 45–53.
[34] D.A. Taylor, B.Z. Atkins, P. Hungspreugs, T.R. Jones, M.C. Reedy, K.A. Hutcheson, D.D. Glower, W.E. Kraus, Regenerating functional myocardium: improved performance after skeletal myoblast transplantation, Nat. Med. 4 (1998) 929–933.
[35] M.H. Soonpaa, G.Y. Koh, M.G. Klug, L.J. Field, Formation of nascent intercalated disks between grafted fetal cardiomyocytes and host myocardium, Science 264 (1994) 98–101.
[36] T. Sakai, R.K. Li, R.D. Weisel, D.A. Mickle, Z.Q. Jia, S. Tomita, E.J. Kim, T.M. Yau, Fetal cell transplantation: a comparison of three cell types, J. Thorac. Cardiovasc. Surg. 118 (1999) 715–724.

Journal of Cellular Biochemistry 90:158–169 (2003)

Differentiation Potential of a Mouse Bone Marrow Stromal Cell Line

Elizabeth H. Allan,[1] Patricia W.M. Ho,[1] Akihro Umezawa,[2] Jun-Ichi Hata,[2] Fusao Makishima,[3] Matthew T. Gillespie,[1] and T. John Martin[1]*

[1]St. Vincent's Institute of Medical Research, 9 Princes Street, Fitzroy, Vic 3065, Australia
[2]Department of Pathology, Keio University, School of Medicine, 35 Shinanomachi, Shinjuku-ku, Tokyo 160-8582, Japan
[3]Fuji Gotemba Research Laboratories, Chugai Pharmaceuticals Co. Ltd., 1-135 Komakado, Gotemba, Shizuoka 412-8513, Japan

Abstract In order to study osteoblast differentiation we subcloned a cell derived from a mouse a bone marrow stromal cell line, Kusa O, and obtained a number of clones representative of three different phenotypes. One that neither differentiated into osteoblasts nor into adipocytes, a second that differentiated into osteoblasts but not adipocytes, and a third that differentiated into both osteoblasts and adipocytes. Four subclones were selected for further characterization according to their ability to mineralize and/or differentiate into adipocytes. The non-mineralizing clone had no detectable alkaline phosphatase activity although some alkaline phosphatase mRNA was detected after 21 days in osteoblast differentiating medium. Alkaline phosphatase activity and mRNA in the three mineralizing clones were comparable with the parent clones. Osteocalcin mRNA and protein levels in the non-mineralizing clone were low and non-detectable, respectively, while both were elevated in the parent cells and mineralizing subclones after 21 days in differentiating medium. PTH receptor mRNA and activity increased in the four subclones and parent cells with differentiation. mRNA for two other osteoblast phenotypic markers, osteopontin and bone sialoprotein, were similarly expressed in the parent cells and subclones while mRNAs for the transcription factors, Runx2 and osterix, were detectable in both parent and subclone cells. Runx2 was unchanged with differentiation while osterix was increased. Interestingly, PPARγ mRNA expression did not correlate with cell line potential to differentiate into adipocytes. Indian hedgehog mRNA and its receptor (patched) mRNA levels both increased with differentiation while mRNA levels of the Wnt pathway components β-catenin and dickkopf also increased with differentiation. Although we have focussed on characterizing these clones from the osteoblast perspective it is clear that they may be useful for studying both osteoblast and adipocyte differentiation as well as their transdifferentiation. J. Cell. Biochem. 90: 158–169, 2003.

Key words: stromal cells; osteoblasts; adipocytes; differentiation; plasticity

Multipotential stromal stem cells from the bone marrow can differentiate into a number of cell types including osteoblasts, adipocytes, reticulocytes, and fibroblasts [Owen, 1985]; the progenitors of which have the ability to transdifferentiate [Beresford et al., 1992; Oreffo et al., 1997]. Osteoblast differentiation of these cultures is dependent upon the addition of ascorbate, which stimulates the synthesis of collagen followed by induction of osteoblastic genes [Franceschi et al., 1994]. Commitment to and interconversion of stromal cells among the several phenotypes is likely to involve specific genes that may be required to induce or suppress a particular phenotype.

It is now well documented that the transcription factor, Runx2, is required for commitment to the osteoblast phenotype [Ducy et al., 1997] and that in Runx2 null mice osteoblast differentiation is arrested in both the endochondrial and intramembranous skeleton [Komori et al., 1997; Otto et al., 1997]. Runx2 is known to

Grant sponsor: NHMRC Program; Grant number: 003211; Grant sponsor: Chugai Pharmaceutical Co., Japan.

*Correspondence to: Professor T. John Martin, St. Vincent's Institute of Medical Research, 9 Princes Street, Fitzroy, Vic 3065, Australia. E-mail: thomasjm@unimelb.edu.au

Received 14 April 2003; Accepted 10 June 2003
DOI 10.1002/jcb.10614

modulate the transcription of several genes involved in the mineralization process. The bone sialoprotein (BSP) promoter has a number of functional Runx DNA binding sites and Runx2 mediates repression of the promoter [Javed et al., 2001]. In contrast, Runx2 enhances transcription of both type1 collagen genes [Kern et al., 2001], collagenase 3 [Jiménez et al., 1999], osteoprotegerin [Thirunavukkarasu et al., 2000], osteopontin [Sato et al., 1998], and osteocalcin [Gutierrez et al., 2002]. Furthermore, Runx2 appears to interact synergistically with C/ERPβ, enhancing transcription of osteocalcin 30–40-fold in HeLa cells co-expressing Runx2 and C/ERPβ compared with 2–4-fold for each protein alone [Gutierrez et al., 2002]. Another transcription factor essential for osteoblast differentiation is osterix. This factor appears to be required at a later stage of differentiation than Runx2 since preosteoblasts of osterix null mice express Runx2 at comparable levels to wild type osteoblasts while no expression of osterix was apparent in Runx2 mice [Nakashima et al., 2002]. Other transcription factors are involved in commitment of multipotential stromal cells to the adipocytic pathway, of these PPARγ has been reported to have divergent effects on adipocyte and osteoblast differentiation by playing a role in the function of many adipocyte specific genes, such as αP2 and PEPCK, as well as suppression of Runx2 [Lecka-Czernik et al., 1999] and synthesis of α1(1)-procollagen, osteopontin, alkaline phosphatase, and osteocalcin [Lecka-Czernik et al., 2002].

Alkaline phosphatase, osteopontin, BSP, PTH receptor-1 (PTHR1), and osteocalcin are all proteins whose significance in osteoblast differentiation has been studied extensively [Bellows et al., 1991]. Although variation occurs among species and cell types, osteopontin, BSP, PTHR1, and alkaline phosphatase are generally associated with early osteoblasts while osteocalcin is an indicator of the mature osteoblast [Aubin, 1998] and is implicated in the inhibition of the mineralization process [Ducy et al., 1996]. In the last few years, new insights into osteoblast differentiation have been provided by the discovery of several new transcription factors and signaling pathways. The present work was undertaken to identify cells in which osteoblast differentiation could be studied in vitro, with the aim of putting the new control pathways into context with what was known previously.

Kusa O cells are a subclone of Kusa cells that were cloned from mouse bone marrow stromal cells and which differentiate into osteoblasts, adipocytes, and myoblasts [Umezawa et al., 1992]. The Kusa O cells demonstrated plasticity and were found to support osteoclastogenesis [Horwood et al., 1998]. When incubated in the presence of ascorbate and β-glycerophosphate, a subpopulation developed an osteoblastic phenotype and formed mineralized nodules while another developed an adipocytic phenotype. We therefore subcloned the Kusa O cells with the view to obtaining genetically related clones with different phenotypes.

MATERIALS AND METHODS

Cell Culture

Kusa O cells were derived from a multipotential bone marrow stromal cell line [Umezawa et al., 1992] and were maintained in α-modified Eagle's minimal medium (αMEM) plus 10% FCS. Subclones were obtained by limiting dilution and frozen at passage 3. Cells were used between passages 5 and 20 and maintained in the same medium as the parent Kusa O cells. The characteristics of the clones appeared stable up to 25 passages, thereafter the mineralizing clones lost their capacity to mineralize.

Bone Nodule Assay

Cells were subcultured at a density of 3,000 cells/cm^2 in αMEM plus 10% FCS for 24 h before changing to an osteoblast differentiating medium of αMEM plus 15% heat-inactivated FCS (HIFCS) together with ascorbate and β-glycerophosphate (50 μg/ml and 10 mM, respectively). Cells were maintained in this medium for the times indicated and the medium was replaced three times a week. At the end of the incubation, the cells were washed three times in PBS, fixed in ice cold 70% ETOH for 1 h, and stained with 0.5% alizarin red pH 4.2 for 30 min. Cells were washed three times with deionized water and twice with PBS for 10 min. Alizarin red was eluted in 10% cetylpyridinium chloride in PBS and measured spectrophotometrically as described by Stanford et al. [1995].

Oil Red-O Lipid Staining

Cells were cultured in an adipocyte differentiating medium (6.6×10^{-8} M insulin, 2.5×10^{-10} M 3-isobutyl-1-methylxanthine,

and 10^{-8} M dexamethasone) with medium changes three times a week. Cultures were washed and fixed as for the nodule assay before staining for lipid by the Oil Red-O method [Kuri-Haruch and Green, 1978].

Alkaline Phosphatase Assay

Cells were washed three times with PBS, scraped in ice cold 10 mM Tris HCl, pH 7.4, sonicated for 10 s on ice, and stored at −20°C until assayed. Extracts were assayed for alkaline phosphatase activity at 37°C for 30 min using *p*-nitrophenyl-phosphate as substrate [Partridge et al., 1981]. Aliquots of the cell extracts were assayed for protein using a BCA protein assay kit (Pierce, Milwaukee, WI).

PTH/PTHrP Receptor

Cells were subcultured and incubated as for the nodule assay for 7 or 21 days with the exception that no β-glycerophosphate was added to the medium. At the end of the incubation, cells were treated with 10 nM PTH (1–34) in the presence of isobutylmethylxanthine and cyclic AMP formation assayed as described by Houssami et al. [1994].

PTHrP and Osteocalcin Protein

Cells were subcultured at the same density as for the nodule assay. After 24 h, the medium was replaced with αMEM plus 15% HIFCS and 50 μg/ml ascorbate, and cells were incubated for 7 or 21 days. Three days prior to sample collection, the medium was replaced with αMEM plus 2% FCS together with ascorbate (50 μg/ml). At the end of the incubation time, the medium was aspirated, centrifugued briefly to remove any cell debris, and supernatants stored at −20°C until assayed for PTHrP by radioimmunoassay [Grill et al., 1991] or osteocalcin using an ELISA for rat osteocalcin (Osteometer BioTech A/S, Herlev, Denmark). The cells were washed, extracts prepared as for alkaline phosphatase measurements and assayed for protein using a BCA protein assay kit (as described above).

Gene Expression Analysis by Real-Time PCR

Cells were subcultured at the same density as for the nodule assay. After 24 h, the medium was aspirated and replaced with αMEM plus 15% HIFCS for the zero time cultures while ascorbate (50 μg/ml) was added to cultures which were examined after growth for 7 and 21 days. Zero time samples were lysed when cultures were just confluent while the 7 and 21 day cultures were lysed 7 and 21 days after the addition of ascorbate. Total RNA was prepared according to the method of Chomczynski and Sacchi [1987] and treated with DNase to remove any contaminating DNA. RNA was reversed transcribed using random hexamers and AMV reverse transcriptase. Authenticity of product was assessed for each primer pair according to size and by hybridizing the PCR product with an internal oligonucleotide probe. Aliquots of the RT mix were diluted so that they fell within the linear portion of the standard curve generated from dilutions of cDNA. All PCR reactions were performed in duplicate and the mean cycle threshold values were used to calculate gene expression with normalization to 18s. Results are represenative of three independent experiments. Amplification was carried out using AmpliTaq Gold (Perkin-Elmer) with SYBR Green (Molecular Probes) as probe and specific oligonucleotide primers (Table I). Cycling conditions were 95°C for 15 s, 60°C for 60 s for 40 cycles in a GeneAmp 5700 Detection System (Perkin-Elmer Applied Biosystems, Inc.).

RESULTS

Mineralization of Subclones

Of 10 clones that were obtained by subcloning the Kusa O cells, 4 that were representative of clones that had different osteoblastic and adipocytic potential were selected for the study. Figure 1 shows mineralization and lipid formation in these clones together with the parent Kusa O cells. The Kusa O cells could form mineralized nodules and adipocytes, Kusa4d10 failed to form mineralized nodules or adipocytes, Kusa4b10 formed mineralized nodules but failed to differentiate into adipocytes in osteoblast differentiating medium although small numbers were apparent in cultures incubated in adipocyte differentiating medium as shown in the Figure 1. The remaining two clones, Kusa1c11 and Kusa2g11, like the parent Kusa O cells, formed large numbers of mineralized nodules and differentiated into adipocytes in both osteoblast differentiating medium and adipocyte differentiating medium.

Comparison of the osteoblast phenotype of the four subclones with the parent Kusa O cells is illustrated in Figure 2. Mineralization first became apparent around day 15 and increased

TABLE I. Primers Used in Real Time PCR Analysis of Mouse Reverse Transcribed RNA

Gene	Sequence	
	5′f	5′r
Alkaline phosphatase	aaa ccc aga aca caa gca ttc c	tcc acc agc aag aag aag cc
BSP	cga tca gaa aaa gca gca cc	gta gcc ttc ata gcc atg cc
β-Catenin	agc tgg cct ggt ttg ata c	aaa acc att ccc acc cta c
Dickkopf	gac cac agc cat ttt cct c	tgt ctt gca caa cac agc c
Indian hedgehog	gga gac acc att gag act tga a	tga aga atc gca gcc aga g
Lrp5	gga ctt cat cta ctg gac cga c	tgc acc ctc cat ttc cat c
Osteocalcin	tct ctc tga cct cac aga tcc c	tac ctt att gcc ctc ctg ctt g
Osteopontin	cca tct cag aag cag aat ctc c	atg gtc atc atc gtc gtc c
Osterix	tat gct ccg acc tcc tca ac	aat agg att ggg aag cag aaa g
Patched	caa act ttg acc cct tgg aa	aaa aca agg ggc aca tca ag
PPARγ	gga aag aca acg gac aaa tca c	tac gga tcg aaa ctg gca c
PTHR	ttc cag gga ttt ttt gtt gc	agt cca tgc cag tgt cca g
Runx2	ctc cgc tgt gaa aaa cc	tga aac tct tgc ctc gtc c
Smoothened	cag gag ctc tcc ttc agc at	ttg ttc ttc tgg tgg cac tg
18s	cga tgc tct tag ctg agt gt	ggt cca aga att tca cct ct

rapidly over 28 days in all but the Kusa4d10 subclone (Fig. 2A). Alkaline phosphatase activity was indicative of mineralization capacity, with clones Kusa4b10, Kusa1c11, and Kusa2g11 showing that increasing alkaline phosphatase activity preceded mineralization (Fig. 2B). No alkaline phosphatase activity was detected in the non-mineralizing Kusa4d10 clone by this assay. Osteocalcin protein, a late marker of the osteoblast phenotype, was undetectable at day 7 but expressed by day 21 in all but the non-mineralizing Kusa4d10 cells (Fig. 2C). PTHrP was not detected in the medium from any of the clones at day 7 but was detected by day 21 in clones Kusa4b10, Kusa1c11, and Kusa2g11 but not in the Kusa4d10 cells or surprisingly the parent Kusa O cells (Fig. 2D). Induction of the PTH receptor was not apparent at day 7 but by day 21 the parent cells and four subclones demonstrated considerable PTH responsiveness (Fig. 2E).

Messenger RNA levels of the osteoblastic markers measured in Figure 2 as well as osteopontin and BSP were detected by quantitative RT-PCR. Alkaline phosphatase mRNA (Fig. 3A) expression increased with differentiation in the Kusa O, Kusa1c11 and Kusa2g11 cells, while the level in the Kusa4b10 cells appeared to peak earlier in the process and decline at 21 days although the level was still higher than for the other clones. A low level of alkaline phosphatase mRNA was detectable at 21 days in the Kusa4d10 cells and although no activity was detected by the alkaline phosphatase assay (Fig. 2A), a small number of cells stained for alkaline phosphatase in parallel experiments (data not shown). Osteocalcin mRNA (Fig. 3B) was not detectable at 0 and 7 days but was highly expressed on day 21 in all but the Kusa4d10 cells, results that are in agreement with the osteocalcin protein (Fig. 2C). PTHR-1 mRNA (Fig. 3C) was very low in the undifferentiated cells but was highly expressed on day 21, data that were also reflective of the measurement of receptor activity (Fig. 2E). BSP mRNA (Fig. 3D) levels rose dramatically between days 7 and 21 in the Kusa O cells, the subclones and the primary osteoblasts, although the level of BSP mRNA in the Kusa4d10 cells was lower than in the other cells. Osteopontin mRNA (Fig. 3E) levels were low in the non-differentiated cells, but were elevated early in the process, consistent with published data [Aubin, 1998]. These levels were further elevated in the Kusa1c11 and Kusa2g11 clones at 21 days.

Having established a phenotypic profile for the Kusa O cells and four subclones we proceeded to measure mRNA levels of three transcription factors known to regulate expression of the osteoblastic and adipocytic genes. Runx2 mRNA expression did not vary substantially with differentiation or between clones and cultures of primary mouse calvarial osteoblast-like cells (Fig. 4A). Osterix, involved later in differentiation than Runx2, was more highly expressed in more differentiated cells. At 21 days osterix (Fig. 3B) expression in the Kusa4d10 cells was lower than for the Kusa O cells and other subclones but was comparable to the levels in the primary osteoblasts and was still higher than in the undifferentiated cells.